Merseburg University of

Applied Sciences

Program: Sustainable process engineering and chemistry

Synthesis and characterization of triphenyl(2-/3-/4-anisole)tin(IV) complexes

Masterthesis

for attaining the academic degree

Master of Engineering (M.Eng.)

submitted by

Sascha Corvin Schneeweiß

Merseburg, 9th of July 2025

1st Referee: Prof. Dr. h.c. Dr. rer. nat. habil. Goran Kaluđerović

2nd Referee: M.Sc. Slađana Kovačević

To my grandfather,
Günter Willy Kurt Herrmann,
who died of lung cancer.
His strength and faith in me deeply inspired me.
He lives on in my thoughts and in this work.

Acknowledgement

I would like to thank everyone who has supported me in writing this thesis and for their assistance with my lab work. Be it through scientific guidance or words of encouragement.

My sincerest thanks goes to Prof. Dr. Dr. G. Kaluđerović for his excellent supervision of my Master's thesis. I am particularly grateful for his insightful suggestions, his constructive feedback and also his scientific and practical guidance in the laboratory.

I would also like to take this opportunity to thank Ms. S. Kovačević for her support during my laboratory work and during the writing process. I also greatly appreciate the many pieces of advice I was given during my work.

I would also like to thank all my colleagues from Prof. Dr Dr G. Kaluđerović's working group for their support during the syntheses and analyses. I would especially like to thank Mrs Wusterhausen for her constant advice in the laboratory.

Finally, my deepest thanks go to my parents, as they my studies possible in the first place and have supported me throughout my academic journey by always encouraging and challenging me to stay positive and proactive.

Sascha Corvin Schneeweiß

Merseburg, 9th of July 2025

Statement of Authorship

I hereby declare that I have written this paper independently and have not used any sources other than those indicated. All direct and indirect quotations are clearly marked with precise references to the source.

Location and Date

Sascha Corvin Schneeweiß

I Table of contents

II List of Figures

III List of Figures in Appendix

IV List of Schemes

V List of Abbreviations

DNA	deoxyribonucleic acid
NMR	nuclear magnetic resonance
TPTC	triphenyltin chloride
[Ph_3Sn(2-MeOPh)]	triphenyl(2-anisole)tin(IV)

$Ph_3Sn(3\text{-}MeOPh)]$	triphenyl(3-anisole)tin(IV)
$[Ph_3Sn(4\text{-}MeOPh)]$	triphenyl(4-anisole)tin(IV)
Cisplatin	*cis*-diamminedichloridoplatinum(II)
TLC	thin layer chromatography
2-MeOPh	2-anisole, 2-methoxybenzene
3-MeOPh	3-anisole, 3-methoxybenzene
4-MeOPh	4-anisole, 4-methoxybenzene
DEPT	distortionless enhancement by polarisation transfer

Abstract

This study focuses on the synthesis and thorough structural analysis of three organotin(IV) complexes: triphenyl(2-/3-/4-anisole)tin(IV). Due to the high biological activity and associated cytotoxic potential of triphenyltin(IV) compounds represent promising candidates as alternatives to platinum-based chemotherapeutic agents**.** These complexes were synthesised via a modified Grignard reaction, using triphenyltin(IV) chloride and various bromoanisole isomers as the starting materials. The structures of obtained complexes were elucidated using spectroscopic analysis, including multi-nuclear NMR (^{1}H-, ^{13}C-, ^{13}C-DEPT-135- and ^{119}Sn-NMR) and infrared spectroscopy. This analysis confirmed the success of the syntheses. Additionally, the ^{119}Sn NMR shows that all three complexes have a coordination number four, thus tin(IV) centrum is in tetrahedral geometry. An elemental analysis was performed to confirm the purity of the complexes. This work fills a gap in the current literature regarding the synthesis and characterization of triphenyl(anisole)tin(IV) complexes and provides a foundation for further biological evaluation.

1. Introduction

1.1 General Introduction

The inhibitory effect of cisplatin on cell division was first demonstrated by Barnett Rosenberg in 1960s. [1,2] After more detailed investigations, however, cisplatin was found to have several side effects, which served as the basis for further developments in anticancer therapy. The most serious side effects associated with cisplatin use include high nephrotoxicity, cumulative peripheral sensory neuropathy, ototoxicity resulting from irreversible damage to the hair cells of the organ of Corti, as well as nausea and vomiting. The accidental discovery of cisplatin and its mode of action thus marked the beginning of research into metal-based anticancer drugs. [3,4]

Due to the strong side effects of cisplatin, it was decided to retain the general structure of cisplatin, but in some research also to replace platinum with a different metal. The aim was to retain the high efficacy of cisplatin, while minimising the side effects. One metal that exhibited high biological activity compared to many other metals was tin. However, tin compounds are not only of interest for anticancer therapy due to their high biological activity. Of greater interest is the mechanism of action of tin compounds, as they have an apoptotic effect and thus render the cells harmless. [5,6] The important point here is that apoptosis is a form of programmed cell death, which is characterised by the fact that the cell membrane remains intact with the formation of apoptotic bodies when the cell dies. This means that no inflammation can occur, as is the case with necrosis. This type of cell death is therefore highly relevant for drugs in anticancer therapy. [7,8]

However, tin compounds or more precisely organotin(IV) compounds have been known to be effective against malignant cells since 1929. The only problem was that the antiproliferative properties were not known until 1980, when the field of organotin(IV) compounds gained great interest. [6,7] Due to the increased interest in this field, it also turned out that triorganotin(IV) compounds have a clearer efficacy against malignant cells than di- or monoorganotin(IV) compounds. This significantly stronger efficacy against malignant cells is based on the possibility of binding with proteins. Consequently, there is great interest in researching further triorganotin(IV) compounds. With triphenyltin(IV) compounds proving to be particularly interesting candidates in anticancer therapy. [9,10]

1.2 Theoretical Background

1.2.1 Chemistry of Anticancer Drugs

Cisplatin is the most widely used cancer drug and therefore also the best known, which means that its mechanism of action has been well researched over the years. [8] The high effectiveness against malignant cells and the many side effects of cisplatin are since it binds to DNA and forms covalent cross-links. Platinum in the form of Pt(II) mainly binds to the nucleic bases guanine and adenine. This distorts the helical structure of the DNA, leading to inhibition of DNA replication, inhibition of transcription and finally to apoptosis. Figure 1 shows the binding of cisplatin to the DNA strand. [11,12]

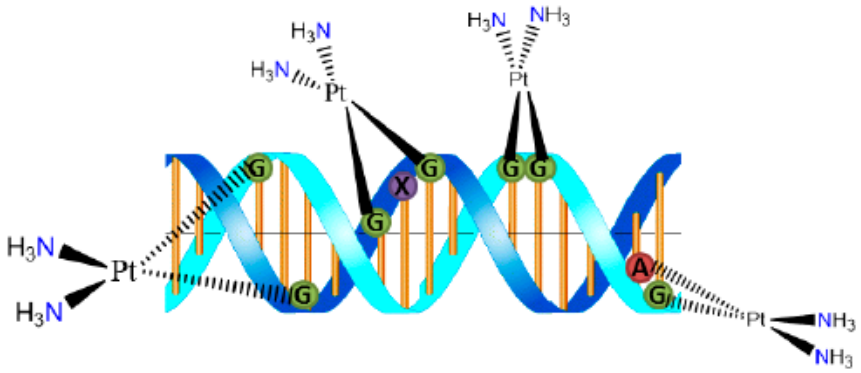

Figure 1: Exemplary binding of cisplatin to DNA [11]

Due to the high efficacy of cisplatin against malignant cells, there is great interest in researching other platinum-based cancer drugs, despite the many side effects. The second generation of platinum-based cancer drugs consists out of carboplatin. Carboplatin exhibits low nephrotoxicity but increased myelotoxicity. [2,9] Figure 2 shows the structure of carboplatin.

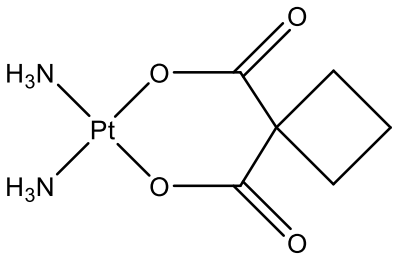

Figure 2: Structure of carboplatin

Whereby the third generation of platinum-based cancer drugs is represented by oxaliplatin, spiroplatin and iproplatin. Oxaliplatin was designed to counteract resistance to cisplatin and carboplatin, while spiroplatin and iproplatin generally have lower toxicity and the human body is less likely to develop resistance to them. Figure 3 shows the structures of oxaliplatin (I), spiroplatin (II) and iproplatin (III). [2,3,13]

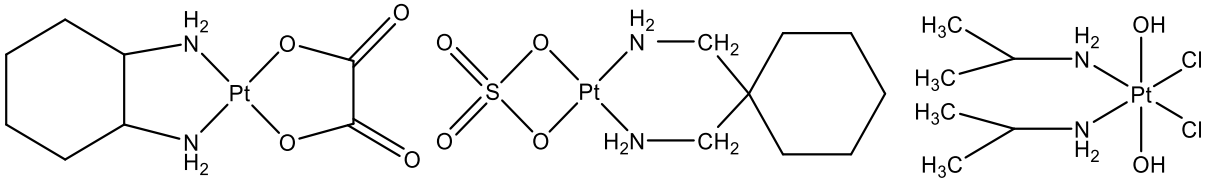

Figure 3: Overview of third-generation platinum complexes

Despite the successes in the treatment of malignant cells with platinum-based anticancer drugs, severe side effects continue to occur. This is why other elements such as titanium, gallium, germanium, palladium, gold, cobalt, ruthenium and tin are also being investigated for their effect against malignant cells. [11,14,15]

The first organometallic substance, besides platinum-based anticancer drugs, to reach clinical trials was budotitanium. Although the applications of the substance are limited by its poor solubility in water and high liver toxicity. [10,11] In order to counteract the poor water solubility or hydrolysis of the titanium complex, titanium(IV) can be bound to cyclopentadienyl ligands. Whereby the resulting titanocene complex has a higher hydrolytic stability. It was on this basis that the working group led by Köpf-Maier and Köpf first began to investigate and characterise these complexes in 1980. [2] Over the decades, the findings of Köpf-Maier and Köpf were used to synthesise and characterise further titanocene complexes, as was done for instance by the working groups of Gomez-Ruiz and Kaluđerović. [11]

In addition to titanocene, gallium complexes (in the form of gallium(III)) are important, as gallium(III) can be absorbed into the body via transferrin due to its similarity to iron(III). In addition, gallium(III) complexes have an antiproliferative effect by inhibiting the enzyme ribonucleotide reductase. As a result, gallium(III) nitrates are currently (as of 2017) undergoing clinical trials for bladder carcinomas and lymphomas. However, the main problem with gallium(III) complexes is their low solubility in biological media. [11]

Furthermore, tin(IV) complexes also have a high cytotoxic effect, often higher than cisplatin, and are also able to overcome the multidrug resistance that has existed to date. In addition to that, medical applications can be enhanced by integrating tin(IV) complexes into silica nanoparticles. Several ligand systems, such as carboxylates, thiolates and cyclopentadienyl derivatives have already been investigated during studies on tin(IV) complexes, with these exhibiting high cytotoxic activities. [10] A more detailed description of the tin(IV) complexes in the form of triphenyltin(IV) complexes is given in section "1.2.2 Chemistry of triphenyltin(IV) complexes".

1.2.2 Chemistry of triphenyltin(IV) Complexes

Tin-based complexes were first shown to be effective against malignant cells in 1971 in the form of triphenyltin(IV) acetate. Since then, tin-based anticancer drugs have been continuously investigated, as tin can coordinate very well with a wide variety of organic ligands and is therefore highly adaptable. [12,13] Triphenyltin(IV) complexes bearing as fourth ligand another organic moiety are very promising, as they have a high toxicity against malignant cells due to strong interactions with proteins. [17–19]

A major problem with organotin(IV) complexes is their poor solubility in water, which severely limits their range of applications. In order to solve this problem, the high adaptability can be utilised, whereby carboxylates can be attached to ionic triphenyltin(IV) chloride. Two examples investigated from the literature are the anionic complexes chlorido(triphenyl)tin(IV) bearing *N*-phthaloylglycinato (**1**: [$NHEt_3$][Ph_3SnCl(P-Gly)]) or 1,2,3-benzenetricarboxylato 1,2-anhydride ligands (**2**: [$NHEt_3$][Ph_3SnCl(BTC)]). These two complexes are shown in Figure 4 below. [18]

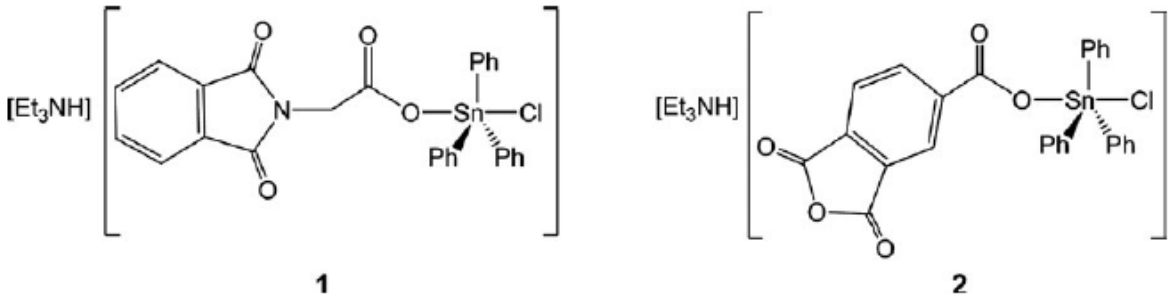

Figure 4: Representation of complexes **1**: [$NHEt_3$][Ph_3SnCl(P-Gly)] and **2**: [$NHEt_3$][Ph_3SnCl(BTC) [18]

These two complexes show high cytotoxicity and also appropriate water solubility. Furthermore, these complexes show a higher selectivity compared to cisplatin, whereby the potential side effects can be greatly minimised. [18]

Other promising candidates are triphenyltin(IV) indomethacinate ([Ph_3Sn(IND)]) and triphenyltin(IV) flurbiprofenate ([Ph_3Sn(FBP)]). Indomethacin was used as a ligand for the synthesis of [Ph_3Sn(IND)] and a racemic flurbiprofen was used for the synthesis of [Ph_3Sn(FBP)] starting from Ph_3SnCl. The structures of both complexes are shown in Figure 5. [15]

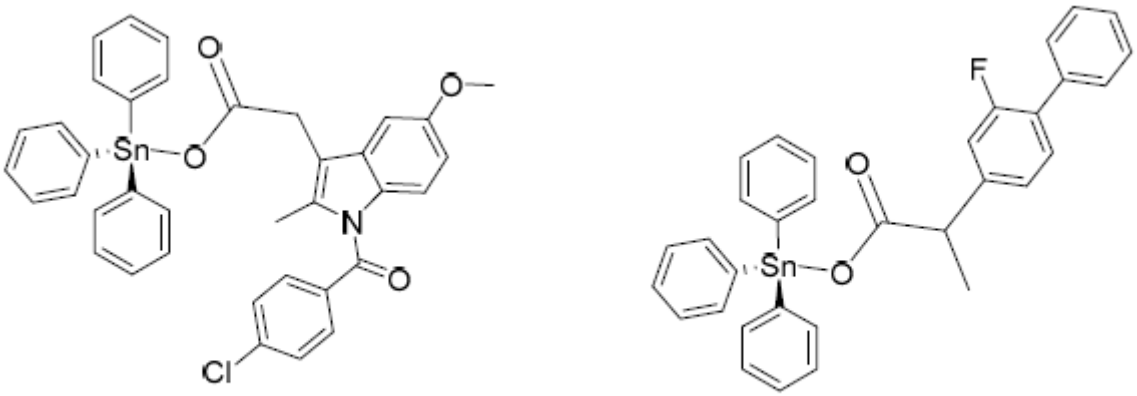

[Ph_3Sn(IND)] [Ph_3Sn(FBP)]

Figure 5: Structures of the complexes [Ph_3Sn(IND)] and [Ph_3Sn(FBP) [15]

Both complexes show high cytotoxic activity against breast cancer cells and differ greatly from cisplatin in their mechanism of action, as no caspase-mediated apoptosis was observed. [15]

1.2.3 Synthesis of triphenyltin(IV) Complexes Bearing Anisole Moiety

Triphenyltin(IV) complexes with an aryl ligand can be synthesised in three different ways. It is not only the reaction pathway that differs, but also instead of the triphenyltin(IV) compound hexaphenylditin(IV), triphenyltin (IV) lithium, triphenyltin (IV) chloride) are used as the starting material. [14,15]

The first synthesis route uses a nucleophile consisting of a triphenyltin(IV) anion and a sodium cation. This can then react with aryl halides to obtain the desired triphenyltin(IV) complex with an aryl ligand. A solution of hexaphenylditin(IV), sodium and liquid ammonia is prepared. This solution is photostimulated in order to slowly add the ligand *p*-iodoanisole, which is pre-dissolved in diethyl ether, in the next step. The reaction solution is then photostimulated for 60 min. After photostimulation, the reaction is terminated with an excess of methyl iodide. The ammonia is then evaporated and benzene is added to dissolve the organic components. The resulting organic solution is filtered and the product triphenyl(4-anisole)tin(IV) is separated by radial TLC. The reaction is shown in the Scheme 1. [14]

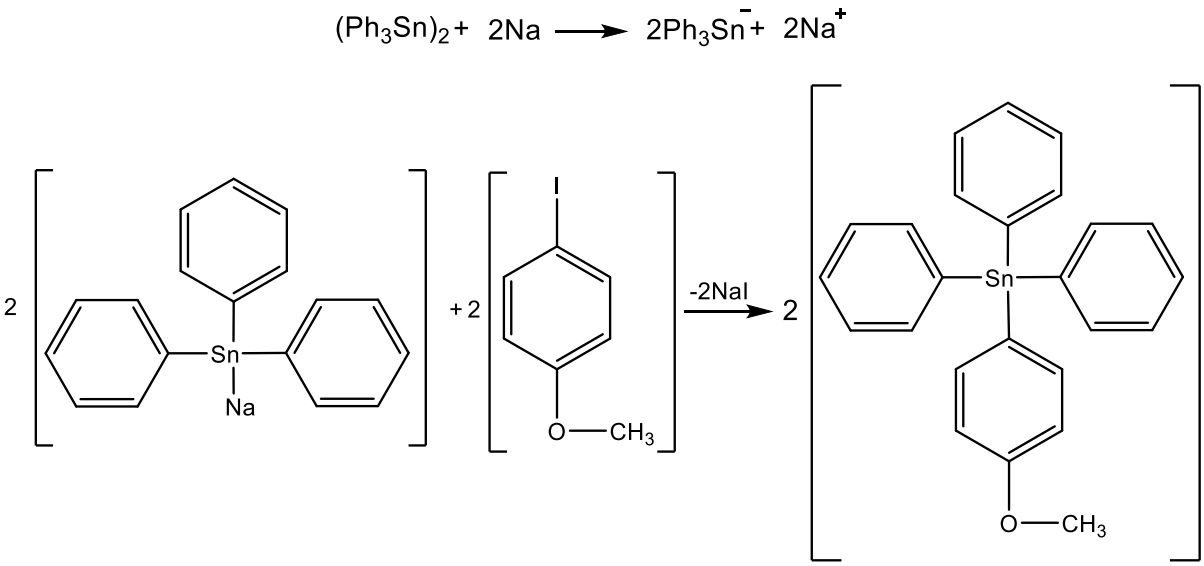

Scheme 1: Synthesis of triphenyltin(IV) sodium and, based on this, the synthesis of triphenyl(4-anisole)tin(IV) [14]

However, the reaction process described above only led to the formation of triphenyl(4-anisole)tin(IV), with no formation of the 2- or 3-anisole derivatives. [14]

Another synthesis route involves the reaction of triphenyltin(IV) lithium with an organic halide. To achieve this, the triphenyltin(IV) lithium is first prepared by pre-dissolving phenyllithium in ether and adding it dropwise to finely ground dry tin(II) chloride. The solution was cooled to -10°C and stirred vigorously. After the addition is complete, the ligand, which is pre-dissolved in diethyl ether, is added in the form of *p*-bromoanisole or *o*-iodoanisole. The solution is then boiled for 18 h under reflux. The reaction-solution is then hydrolysed by transferring it to a saturated ammonium chloride solution, stirring the it vigorously. In the next step, the organic layer is separated and dried with sodium sulphate. The sodium sulphate is th en filtered off so that the dried solution can be evaporated to obtain the solid product. The product was recrystallised from ethanol. The reaction that took place is shown below in Scheme 2. The reaction with *o*-iodoanisole is shown as an example. [15]

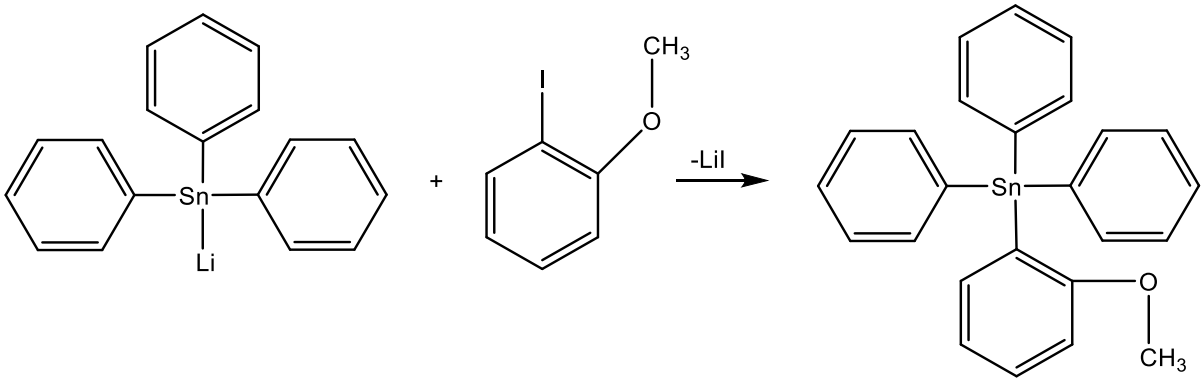

Scheme 2: Synthesis of triphenyl(2-anisole)tin(IV) starting from triphenyltin(IV)-lithium [15]

The third published synthesis route uses triphenyltin(IV) chloride as the starting material. This compound can either react with a Grignard reagent or an organolithium compound. For this reaction, triphenyltin(IV) chloride is dissolved in diethyl ether and *o*-methoxyphenyllithium or *p*-methoxyphenyllithium, which is pre-dissolved in diethyl ether (a Grignard reagent prepared from an *o*-methoxypehnyl compound or a *p*-methoxyphenyl compound can be used instead), is added dropwise. This reaction solution is then refluxed for 1 h and in the next step the solution is transferred to a saturated ammonium chloride solution to terminate the reaction. The organic layer is then separated from the aqueous layer and dried with sodium sulphate, which is then filtered off. The dried solution is then evaporated to obtain an oil. This oil is then refluxed in methanol until it solidifies. The methanol is then decanted off and the solid product (depending on the ligand, triphenyl(2-/4-anisole)tin(IV)) is recrystallised from methanol-benzene (4:1) solution. The reaction is shown below in Scheme 3, as an example for the ligand *ortho*-methoxylithium or the corresponding Grignard reagent (for the Grignard reagent it is assumed that an *ortho*-bromoanisole was used). [15]

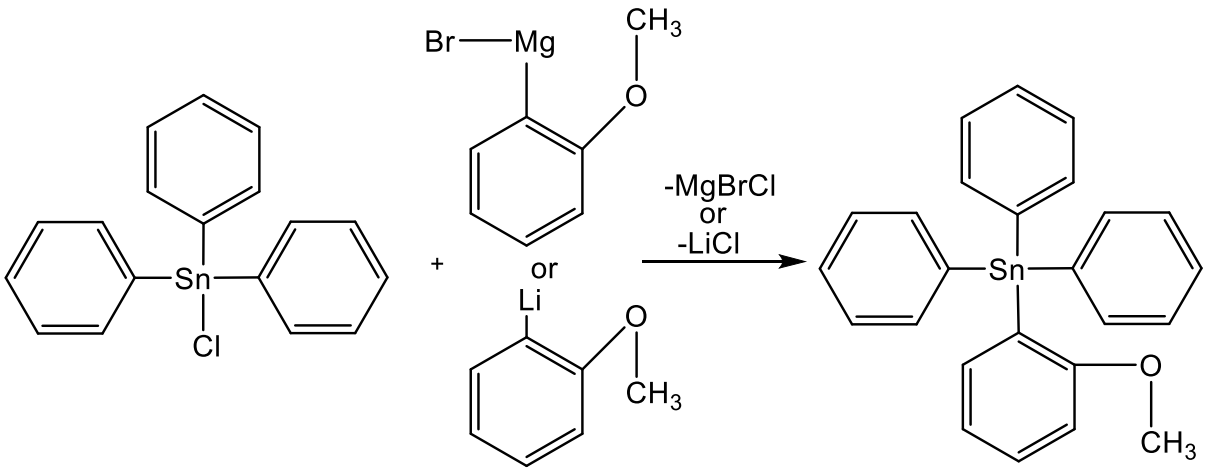

Scheme 3: Synthesis of triphenyltin(2-anisole)tin(IV) starting from triphenyltin chloride and a Grignard reagent or 2-lithium anisole [15]

The problem with synthesis using the Grignard reagent is that no source clearly describes how this Grignard-reagent is obtained, indicating a need for clarification in this regard.

Moreover, no sources describe the synthesis of triphenyl(3-anisole)tin(IV), and a detailed characterisation is lacking for all three triphenyl(2-/3-/4-anisole)tin(IV) complexes.

1.3 Aim of the Master's thesis

Organotin(IV) compounds have different biological properties due to their high adaptability in relation to binding to organic ligands. Depending on the requirements or site of application, different ligands can be used to enhance the effectiveness against malignant cells of the complexes. In this context, organotin(IV) compounds have already been investigated in several *in vivo* and *in vitro* studies and represent a potential alternative for platinum-based anticancer agents. [14,17–19]

The aim of the Master's thesis is to develop new synthesis routes for triphenyl(2-/3-/4-anisole)tin(IV) and to characterise these complexes comprehensively.

Previous gaps in the literature relating to syntheses using Grignard reagents are to be clarified and multinuclear NMR spectroscopy and IR spectroscopy are to be used for characterisation. The synthesised and characterised complexes will be tested for purity using elemental analysis.

2. Results and Discussion

2.1 Synthesis of the [Ph_3Sn(*n*-MeOPh)] (*n* = 2, 3, 4)

For the synthesis of the complexes triphenyl(2-/3-/4-anisole)tin(IV), a synthesis route, already reported for the synthesis of tetrakis(4-methoxybenzene/4-methylbenzene)tin(IV) was adapted and used. [16]

A Grignard reagent is first synthesised using a bromoanisole. Depending on the desired product, 2-bromoanisole, 3-bromoanisole or 4-bromoanisole is used. The chosen compound reacts with magnesium to form the desired Grignard reagent. Before being added, the ligand must be pre-dissolved in diethyl ether, which also serves as the solvent for the entire reaction, and then it should be added very slowly. A catalytic amount of iodine crystals is added to remove the oxide layer of the magnesium surface. This solution is then refluxed for 2 h.

In the next step, the solution is cooled in an ice bath and a theoretically determined amount of triphenyltin(IV) chloride, which has been pre-dissolved in diethyl ether, is added. The amount of triphenyltin(IV) chloride used corresponds to a ratio of 1 equivalent of triphenyltin(IV) chloride to 2.3 equivalents of the bromoanisole ligand. After the addition is complete, the solution is refluxed again for 2 h.

After refluxing, the solution is stirred overnight at room temperature and quenched the next day with 1 M HCl. In the next step, the organic phase is separated from the aqueous phase. The aqueous phase is than washed three times with diethyl ether.

After the organic phases are combined, they are dried over magnesium sulphate, which is then filtered off. The solvent is evaporated under vacuum to yield a white solid. The *n*-hexane is used to remove grease residues, while methanol dissolves remaining reactants and potential side-products.

The reaction is shown in Scheme 4.

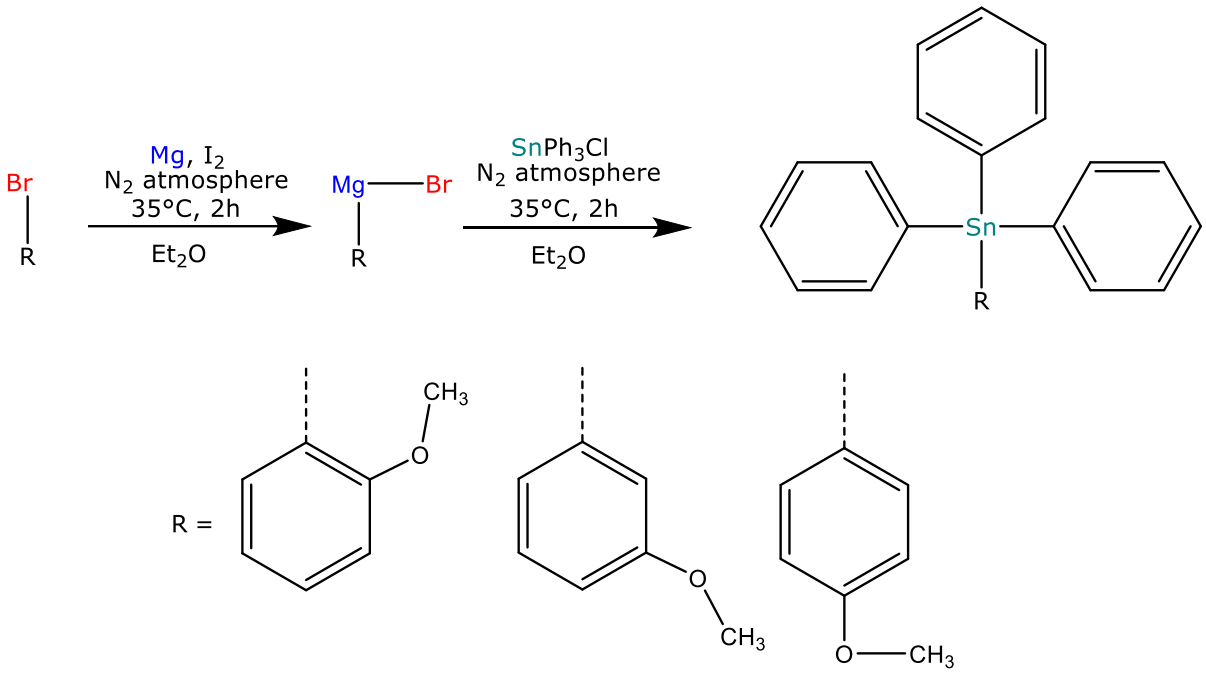

Scheme 4 : Synthesis of the triphenyl(2-/3-/4-anisole)tin(IV) complexes

The success of this synthesis is analysed using ^{1}H-, ^{13}C-, ^{13}C-DEPT-135- and ^{119}Sn-NMR spectroscopy. Furthermore, the purity of the products is ensured by means of elemental analysis.

2.2 Spectral Analysis of the Compounds

2.2.1 Analysis of the ^{1}H-NMR Spectra

In this section, the ^{1}H-NMR spectra of the [Ph_3Sn(*n*-MeOPh)] (*n* = 2, 3, 4) and starting compound [Ph_3SnCl] are presented and analysed. Even thoroughly characterized in the literature [Ph_3SnCl] is used to determine the changes caused by the synthesis and, in connection with this, whether the desired product could be synthesised or whether only the starting material is present.

Figure 6 below shows the ^{1}H-NMR spectrum of [Ph_3SnCl]. Part of the spectrum in the aromatic region relieved characteristic pattern with visible couplings between ^{1}H and ^{119}Sn nuclei, thus resonances at 7.69 and 7.78 ppm in on the aromatic region. The entire spectrum can be found in section VII Appendix in Figure A1.

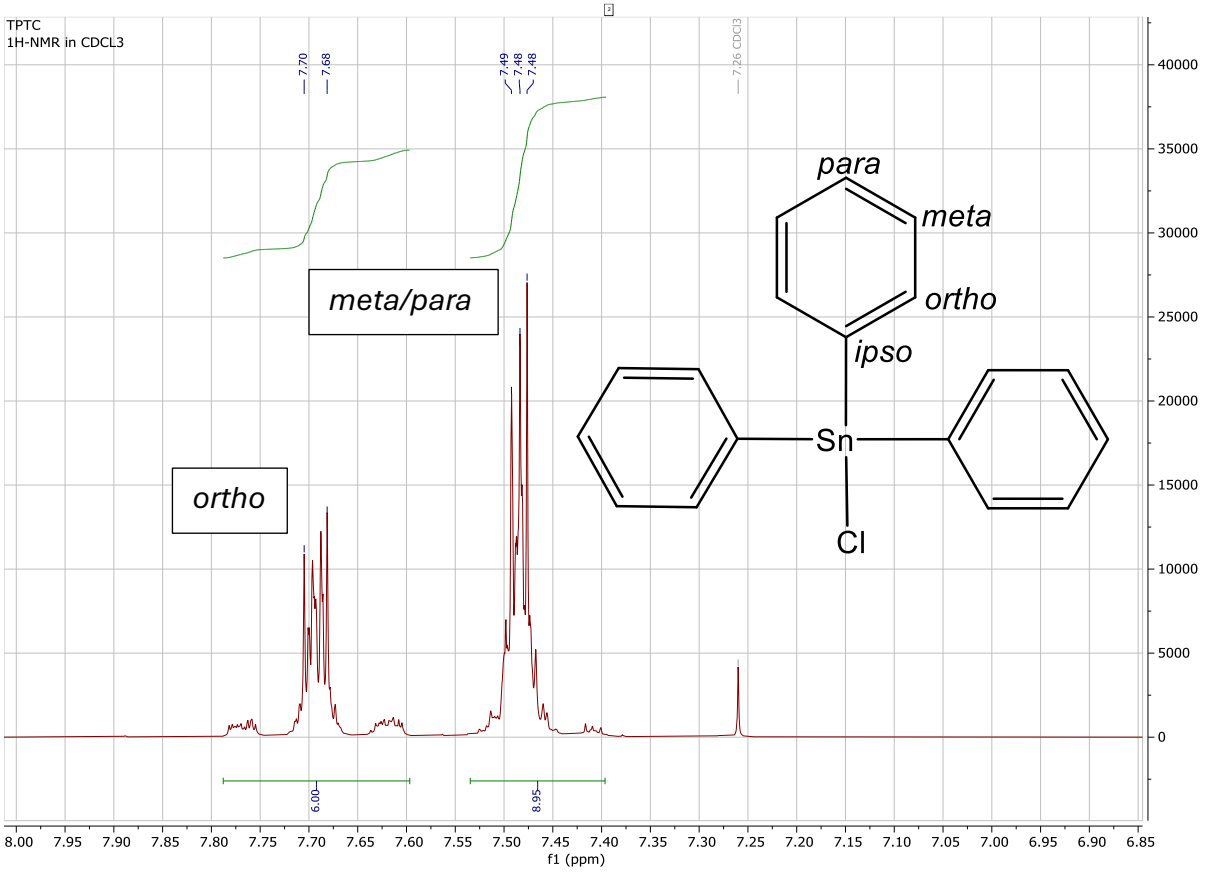

Figure 6: Aromatic region of a ^{1}H-NMR spectrum of TPTC

As can be seen from the structure of the TPTC, the five NMR active hydrogen atoms per phenyl ring are present. The same hydrogen atoms from different phenyl groups are chemically equivalent, and within one phenyl group 3 groups of chemically non-equivalent hydrogen atoms are present. As a result, three resonances of the hydrogen atoms can be detected in the ^{1}H-NMR spectrum. [17]

The resonance at 7.69 ppm can be attributed to C^{ortho}*H* while at 7.48 ppm can be ascribed to C$^{meta/para}$*H*.

In view of the ^{1}H-NMR spectrum in Figure 6, the hydrogen atoms in the *meta* and *para* positions can be assigned to the multiplet at 7.48 ppm, moreoverthe integral of this resonance correspond to 9 H atoms confirming overlapping of mention hydrogen atoms. The main conclusion to be drawn from the integral is that both triplets of the hydrogen atoms in the meta and para positions are so chemically similar that they produce a multiplet in the same chemical shift. These findings are in agreement with interpretations from the literature. [18]

On the other hand, the spectrum shows a multiplet at 7.69 ppm, which has the same integral of six as the hydrogen atoms confirming detection of the ortho hydrogen atoms. However, this multiplet can be also assigned to the hydrogen atoms in the *ortho* position by comparing with the data from the literature. This is further supported by satellite signals, which are caused by the tin isotopes ^{117}Sn and ^{115}Sn. These satellite signals can be recognised in the immediate vicinity of the multiplet. [17,18]

The recognised chemical shifts in the multiplets can be explained by looking at the electron negativities. The carbon atom in the *ipso* position has a higher electron negativity compared to the tin atom. As a result, the carbon atom in the *ipso* position has a slight electron-pulling effect, which slightly increases the electron density of the carbon atom. This also shields the tin atom. In view of this, it can be concluded that the hydrogen atom in the ortho position is more strongly shielded than the hydrogen atoms in the *meta* and *para* positions. [17]

Figure 7 shows the ^{1}H-NMR spectrum and the structure of [Ph_3Sn(2-MeOPh)]. Since most of the important resonances lie in the aromatic region, only this region is shown in Figure 7. The entire spectrum can be found in section VII Appendix in Figure A3. A singlet at 3.75 ppm with an integral of three can be recognised, which (based on literature values) can be assigned to the hydrogen atoms of the methoxy group. [17]

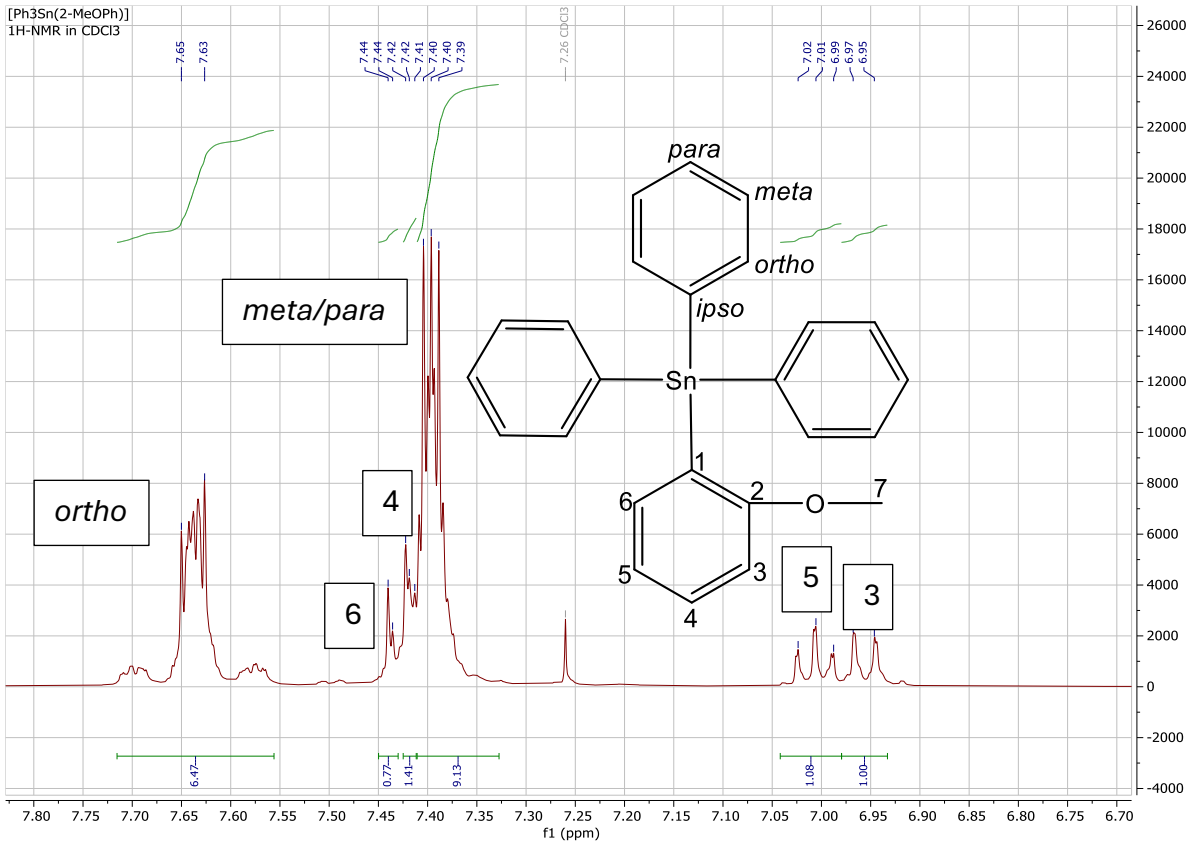

Figure 7: ^{1}H-NMR spectrum and structure of [Ph_3Sn(2-MeOPh)]

It can be seen from the structure in Figure 7 that, just as for the TPTC, three hydrogen atoms of the phenyl rings elicit signals in the aromatic region and for the 2-anisole ligand, four hydrogen atoms exhibit different resonances.

The signal at 7.64 ppm can be attributed to $C^{ortho}H$, the signal at 7.40 ppm can be attributed to $C^{meta/para}H$, the signal at 7.44 ppm can be attributed to $C^{6}H$, the signal at 7.42 ppm can be attributed to $C^{4}H$, the signal at 7.01 ppm can be attributed to $C^{5}H$ *and* the signal at 6.96 ppm can be attributed to $C^{3}H$.

Figure 9 shows the ^{1}H-NMR spectrum and the structure of [Ph_3Sn(3-MeOPh)]. The spectrum only shows the aromatic region, as this is where the most significant signals can be found. In addition to the aromatic region, there is another signal, a singlet, at 3.78 ppm, which can be assigned to the OMe moiety from 3-MeOPh ligand. The entire spectrum can be found in section VII Appendix in Figure A4.

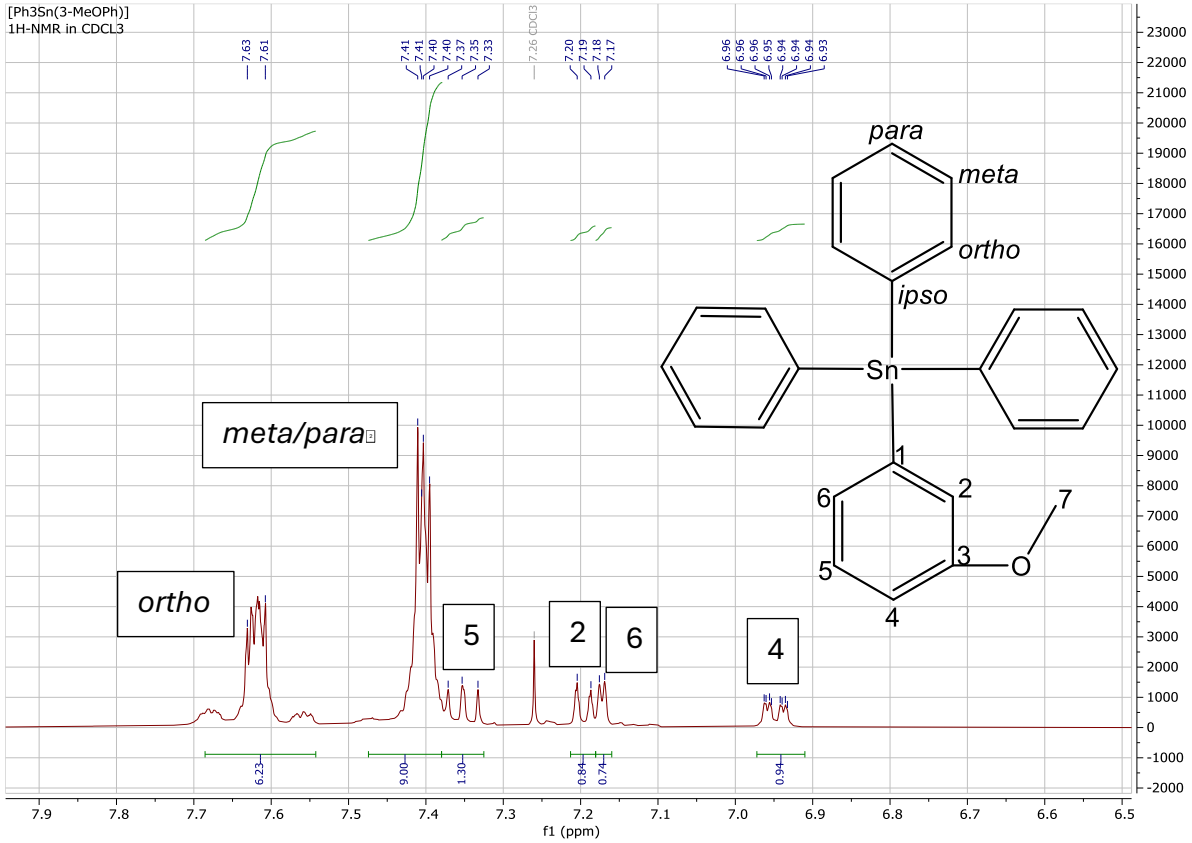

Figure 8: Illustration of the ^{1}H-NMR spectrum and the structure of [Ph_3Sn(3-MeOPh)]

The structure in Figure 8 shows that the [Ph_3Sn(3-MeOPh)] has a total of eight chemically non-equivalent hydrogen atoms. Three hydrogen atoms resonate in a typical region for the Ph groups: 7.62 ppm ($C^{ortho}H$), 7.40 ppm ($C^{meta/para}H$). The resonance at 7.35 ppm can be attributed to $C^{5}H$, while the signal at 7.19 ppm can be ascribed to $C^{2}H$. The $C^{6}H$ and $C^{4}H$ hydrogen atoms are identified at 7.17 ppm and at 6.96 ppm, respectively.

Figure 11 below shows the ^{1}H-NMR spectrum of [Ph_3Sn(4-MeOPh)] and its structure. Figure 11 present only aromatic region in the spectrum while the entire spectrum can be found in section VII Appendix in Figure A5. Outside of the aromatic area is a singlet, which can be recognised at 3.82 ppm and can be assigned to the methoxy group from 4-MeOPh ligand. [17]

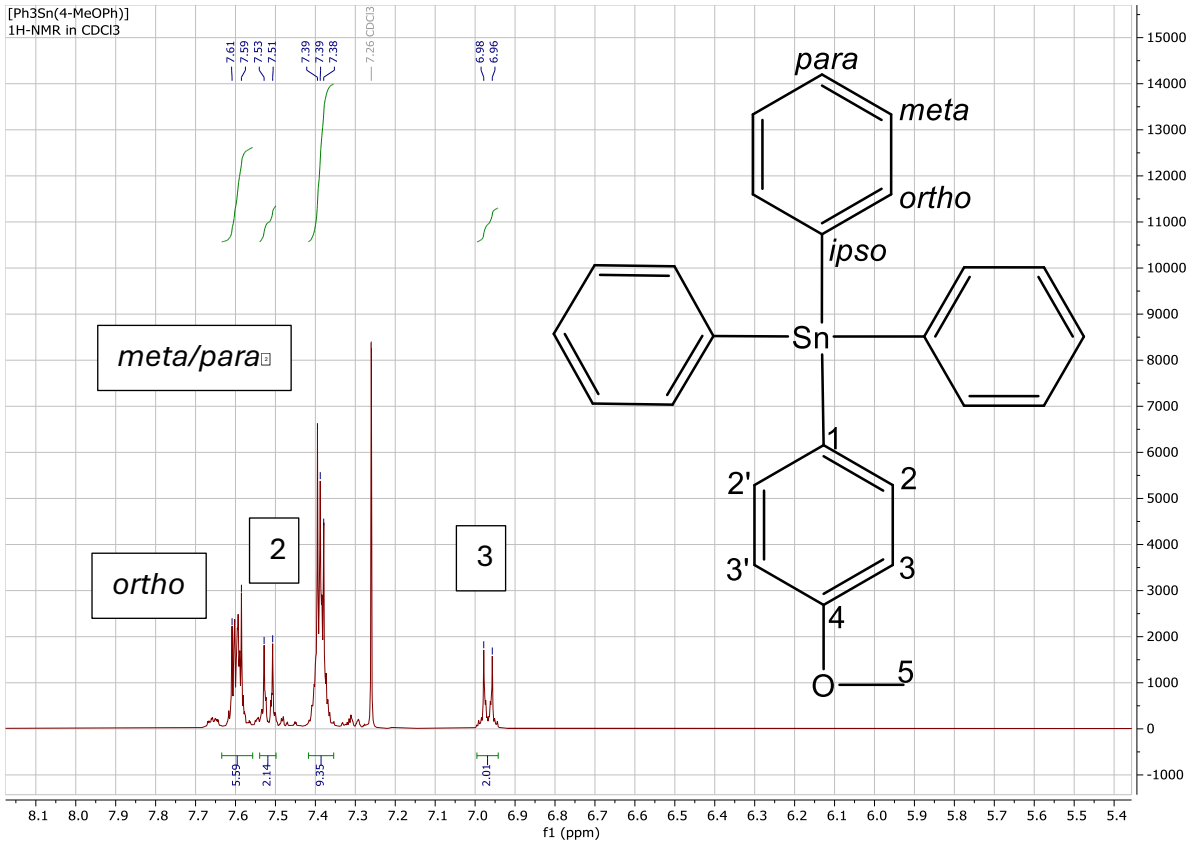

Figure 9: ^{1}H-NMR spectrum and structure of [Ph_3Sn(4-MeOPh)]

According to the structure in Figure 9, it can be concluded that again typical pattern for Ph_3Sn moiety, explicitly hydrogen atoms from Ph fingerprint in aromatic area. Thus resonances at 7.60 ($C^{ortho}H$) and 7.39 ($C^{meta/para}H$) are identified. Due to symmetry in the 4-MeOPh ligand, as expected, only two resonances at 7.52 ppm ($C^{2}H$) and at 6.97 ppm ($C^{3}H$) were detected.

The assignment for the phenyl rings is based on the findings from the analysis of the TPTC. In comparison, it can be recognised that the mutliplet was slightly shielded. The same applies to the triplet, whereby the triplet of the TPTC showed a chemical shift of 7.48 ppm and was also slightly shielded for the [Ph_3Sn(2-MeOPh)]. [17]

In order to be able to assign the multipletts to the hydrogen atoms $C^{3}H$–$C^{6}H$, the different electron negativities must be considered. The carbon atom in the *ipso* position, as for the TPTC, has a higher electron negativity than the tin atom, which means that the carbon atom in the *ipso* position again has a slightly higher electron density. In contrast, the carbon atom in the *ortho* position, which binds directly to the methoxy group, has a lower electron negativity than the oxygen atom of the methoxy group. As a result, the oxygen group has an electron-pulling effect on the carbon atom in the immediate vicinity, which slightly reduces the electron density of the carbon atom and shields the carbon atom. At the same time, however, the electron density of the entire ring, in the 2-anisole ligand, is increased by the positive mesomeric effect of the methoxy group, which also increases its stability. In view of these findings, however, the carbon atom in the C^{1} position has a slightly higher electron density than the carbon atom in the ortho position, which binds to the methoxy group. [17]

In addition, the mesomeric boundary structures can be considered, which are shown in Figure 10 for the 2-anisole ligand.

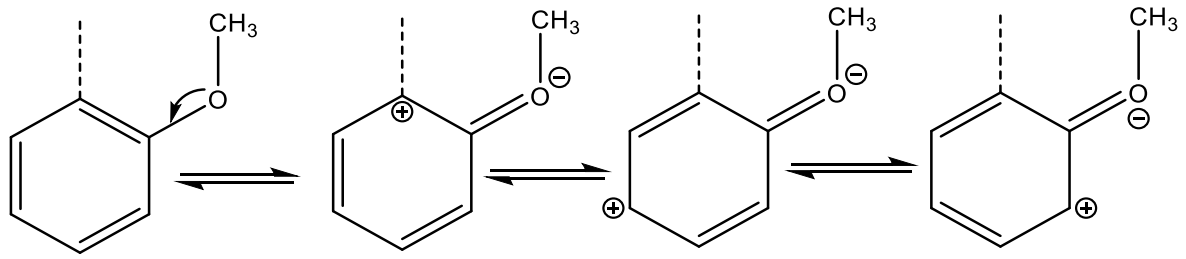

Figure 10: Mesomeric boundary structures of the 2-anisole ligand

It can be recognised that the carbon atoms in the *ipsum* and *meta* positions have a positive charge, whereby the hydrogen atoms that bind to these carbon atoms are deshielded. This affects the C^3H and C^5H hydrogen atoms. As a result, the doublet of the hydrogen atom C^3H can be assigned to the resonance at 6.96 ppm. In addition, the doublet at 6.96 ppm has an integral of 1, which corresponds to the hydrogen atom C^3H. Furthermore, the triplet of hydrogen atom C^5H can be assigned to the chemical shift at 7.01 ppm. In addition, this triplet has an integral of 1, which also corresponds to the C^5H.

The C^4H and C^6H hydrogen atoms, on the other hand, have a stronger shielding, which means that the hydrogen atom C^6H can be assigned to the doublet at 7.44 ppm. In addition, the C^4H hydrogen atom can be assigned to the triplet at 7.42 ppm. [17]

Thus, it can be summarised for the ^{1}H-NMR spectrum of [Ph_3Sn(2-MeOPh)] that all hydrogen atoms could be successfully assigned.

The multiplets of the hydrogen atoms in *meta* and para positions of the Ph moieties are overlapping with the centre of the multiplets at 7.40 ppm, whereby slight differences in the chemical shift can be recognised in comparison to the TPTC. The hydrogen atom in *ortho* can be assigned to the multiplet at 7.62 ppm, like the TPTC, although this multiplet also has a slightly different chemical shift compared to the TPTC. The other hydrogen atoms from 3-anisole moiety, thus C^2H, C^4H–C^6H as well as C^7H_3 resonate in expected range.

In order to determine the multiplicity of the hydrogen atoms of the 3-anisole ligand, the structure is analysed. The hydrogen atom C^4H has only one directly neighbouring hydrogen atom, which is why this hydrogen atom will produce a doublet. This also applies to the hydrogen atom C^6H, which also has only one directly neighbouring hydrogen atom and therefore produces a doublet. In contrast, the hydrogen atom C^5H has two directly neighbouring hydrogen atoms, whereby this hydrogen atom produces a triplet. In contrast, C^7H_3 produces a singlet, as it has no hydrogen atoms in the direct neighbourhood. [17]

To be able to assign these hydrogen atoms, the electron negativity of the tin, the oxygen and the carbon atoms can be used again. The corresponding explanation is the same as already explained for [Ph_3Sn(2-MeOPh)]. To summarise, it can be said that the carbon atom in the C^1 position has a slightly increased electron density and the oxygen atom has an electron-withdrawing effect on the C^3 atom. In addition, the positive mesomeric effect of the methoxy group also has an effect, whereby the aromatic system of the ligand is stabilised and mesomeric boundary structures can be established. These are shown below in Figure 11.

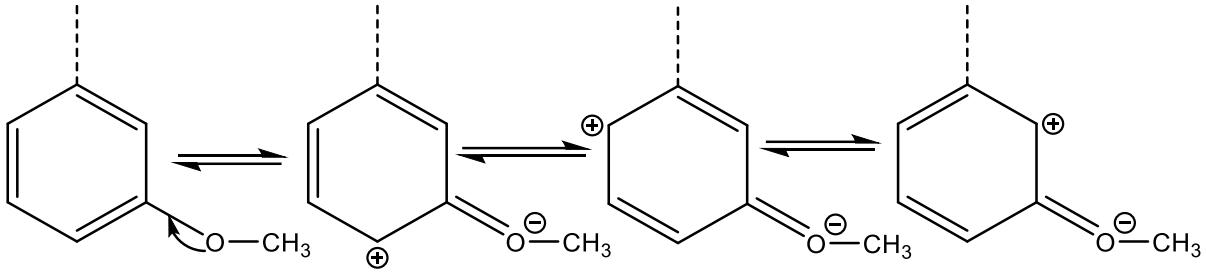

Figure 11: Mesomeric boundary structures for the 3-anisole ligand

According to the mesomeric boundary structures, it can be recognised that the carbon atoms C^2 and C^4 have a positive charge, which shields the signals of the hydrogen atoms bound to them in the ^{1}H-NMR spectrum.

Because the carbon atom C^5 has no positive charge, the hydrogen atom that binds to it C^5H,is the most strongly deshielded. This means that the signal is also more strongly deshielded than the other signals of the 3-anisole ligand. Consequently, the hydrogen atom C^5H can be assigned to the signal at 7.35 ppm. This interpretation is further supported by the multiplicity, as it is a triplet and this triplet has an integral of ca. 1. [17]

Even though the carbon atom C^2 (which binds to the hydrogen atom C^2H) has a positive charge, the associated hydrogen atom is shielded by the increased electron density of the carbon atom in the ipsum position and the methoxy group in relative proximity. In addition to that, this hydrogen atom can enter a remote coupling with the hydrogen atoms C^4H and C^6H. Whereby the signal of the hydrogen atom C^2H would not appear as a pure singlet, but as a kind of pseudo doublet. This applies to the resonance at 7.19 ppm with the integral of ca. 1. [17]

Similar to the hydrogen atom C^2H, the C^6H is also shielded by the slightly increased electron density of the carbon atom C^1, which means that it must have a similar chemical shift to the hydrogen atom C^2H. This applies to the signal with the chemical shift 7.17 ppm. In addition, this resonancel appears as a doublet, which matches the hydrogen atom C^6H. [17]

To support correct assignments of the hydrogen atoms C^2H and C^6H small satellites are identified directly next to mentioned resonances. However, these satellites can only occur if the corresponding hydrogen atom is in proximity (^3J coupling) to the tin atom. Whereby the satellite signals are generated by the isotopes ^{117}Sn and ^{115}Sn. [20]

Because the C^3 carbon atom binds to the oxygen atom has a slightly lower electron density compared to the carbon atom C^1, the hydrogen atom C^4H is the most strongly shielded. It is also the furthest away from the tin atom, which means that it has little or no effect on the chemical shift. In addition, this hydrogen atom can enter remote coupling with the hydrogen atoms C^2H and C^6H , creating a doublet of doublets pattern. This pattern can only be recognised for the resonance at 6.94 ppm, whereby this signal also overlaps with the previously explained interpretations and can therefore be assigned to the hydrogen atom C^4H. Furthermore, this resonance has appropriate integral. [17]

Finally, it can be concluded that [Ph_3Sn(3-MeOPh)] is pure by the sensitivity of ^{1}H NMR measurements To further characterise this complex, a ^{13}C-NMR spectrum and an infrared spectrum were nevertheless recorded.

The assignment of the signals to the hydrogen atoms of the phenyl rings is analogous to the previous samples.

The 4-anisole ligand only elicit two signals (in the aromatic region), as the hydrogen atoms C^2H and $C^{2'}H$ are chemically equivalent and only generate one signal. The same applies to the hydrogen atoms C^3H and $C^{3'}H$. [17]

The assignment of the hydrogen atoms to the doublets is again based on the electron negativity. Analogous to [Ph_3Sn(2-MeOPh)] and [Ph_3Sn(3-MeOPh)], the electron negativities of the tin atom and the neighbouring carbon atom in the C^1 position and of the oxygen atom, the methoxy group, and the neighbouring carbon atom (for [Ph_3Sn(4-MeOPh)], the carbon atom in the C^4 position) are considered. As a result, the carbon atom in the C^1 position again has a slightly higher electron density compared to the carbon atom in the C^4 position. Nevertheless, the aromatic ring is stabilised by the positive mesomeric effect of the methoxy group. The mesomeric boundary structures can also be used for [Ph_3Sn(4-MeOPh)] to show which carbon atom can have a positive charge, whereby the hydrogen atom adjacent to this carbon atom is slightly shielded. Figure 12 below shows the mesomeric boundary structures of the 4-anisole ligand.

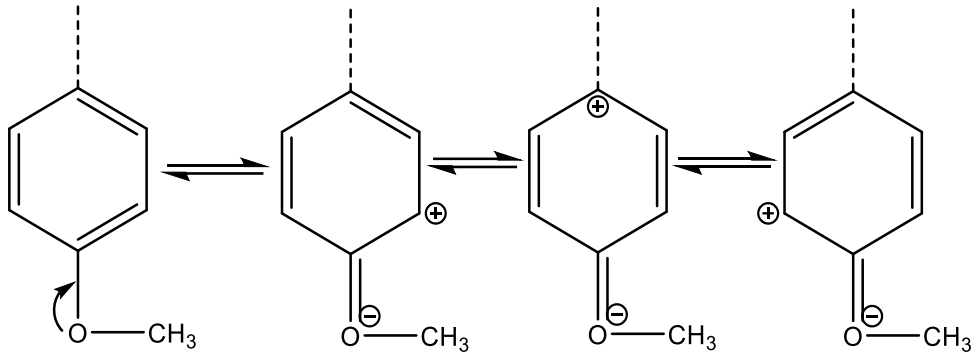

Figure 12: Mesomeric boundary structures of the 4-anisole ligand

According to the mesomeric boundary structures, it can be recognised that the carbon atom in the C^3 position can have a positive charge, which slightly shields the hydrogen atom C^3H. In contrast, the hydrogen atom C^2H is shielded by the slightly increased electron density of the carbon atom in C^1 position. Consequently, the hydrogen atom C^2H can be assigned to the doublet at 7.52 ppm and the hydrogen atom C^3H to the doublet at 6.97 ppm. This conclusion is additionally supported by the fact that the doublet at 7.52 ppm shows satellite signals which can be assigned to the tin isotopes $^{117/115}$Sn. These satellite signals indicate that this doublet must belong to the hydrogen atom C^2H, as its close to the tin atom. [17]

In conclusion, it can be recognised that typical signals for a 4-anisole ligand could be detected, as well as typical signals for a triphenyltin compound. It can therefore be concluded that the complex triphenyl(4-anisole)tin(IV) is present.

2.2.2 Analysis of the ^{13}C-NMR-spectra

In this section, the ^{13}C-NMR spectra will be used to further clarify the sample configuration. In order to be able to make a more precise assignment of the quaternary carbon atoms, ^{13}C-DEPT-135 spectra of the samples are also recorded and analysed.

Analogue to the evaluation of the ^{1}H-NMR spectra, the TPTC is also shown first for the ^{13}C-NMR and ^{13}C-DEPT-135 spectra evaluation so that it can be used for the comparison.

Figure 13 shows the ^{13}C-NMR spectrum of the TPTC. The same sample was used for the measurement as for the ^{1}H-NMR measurement, resulting in a reference solvent signal for the deutero chloroform, a triplet, at 77.16 ppm. Since the spectrum only shows the signals in the aromatic region (except the solvent signal), only the aromatic region is shown in Figure 13. The entire spectrum with the solvent signal can be found in section VII Appendix in Figure A2. [17]

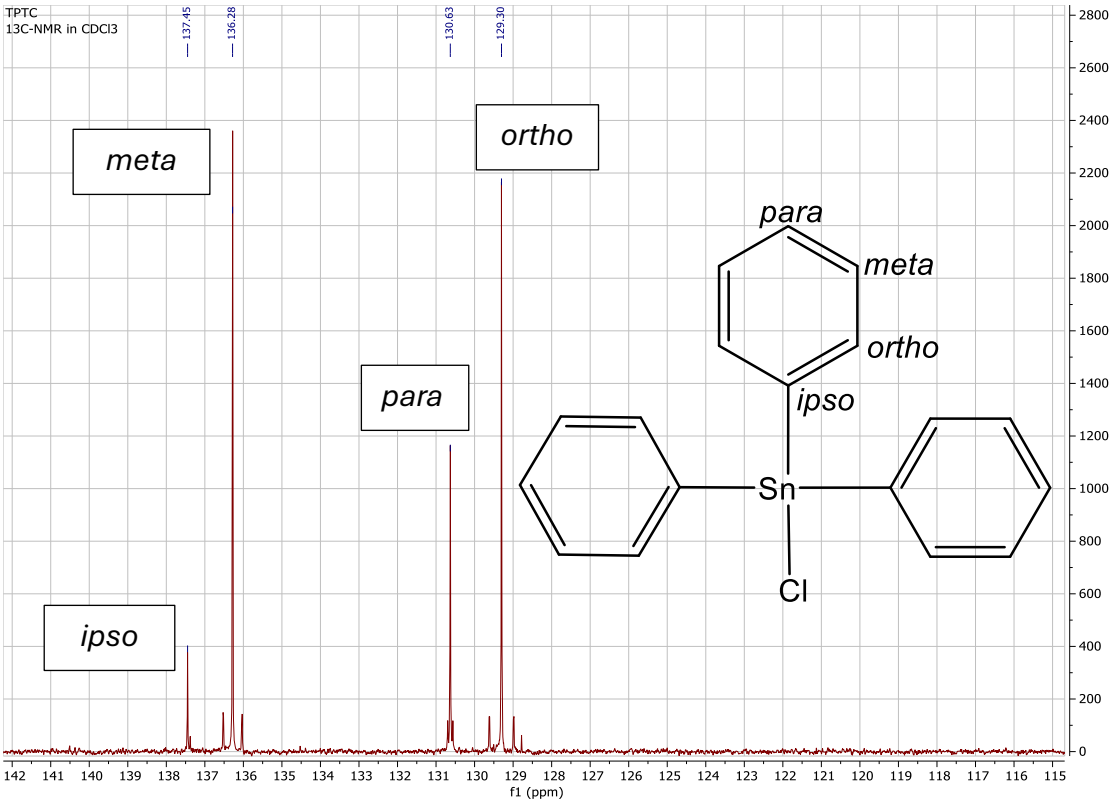

Figure 13: Illustration of the ^{13}C-NMR spectrum of the TPTC

According to the structure of TPTC, each of the phenyl rings has six carbon atoms. Whereby the carbon atoms in the *ortho* position are chemically equivalent to each other and the carbon atoms in the *meta* position also. Consequently the structure generates four resonances in the ^{13}C-NMR spectrum. [17]

It can be recognised from the ^{13}C-NMR spectrum of TPCT (Figure 13) that the signals at 136.28 ppm and 129.30 ppm are of higher intensities than the signals at 137.45 ppm and 130.63 ppm. These more intense signals consist out of more carbon atoms, which means that the *ortho* and *meta* carbon atoms can be assigned to these signals, as the intensity of the signals is amplified by the presence of the chemically equivalent carbon atoms (labelled "*ortho*" and "*meta*"). Consequently, the *ipso* and *para* carbon atoms can be assigned to the signals at 137.45 ppm and 130.63 ppm. [17]

Additionaly, the $^{117/115}$Sn and ^{13}C coupling can be used for assignation of the carbon atoms, whereby the distance between the satellite signals and the actual signal is considered. It should be noted that the satellite signals move further away from the main signal or have a larger coupling constant *J*, the closer the corresponding carbon atom is to the tin atom. This means that the satellite signals for the carbon atom in the *ipso* position are significantly further away than the satellite signals for the carbon atom in the *para* position, when detectable. [17]

It can be seen from the ^{13}C-NMR spectrum in Figure 13 that the signal at 137.45 ppm shows very large coupling constants (J = 293 Hz) assigned to C^{ipso}. In contrast, the signals at the chemical shifts of 136.28, 130.63 and 129.30 ppm with the coupling

constants of 24.2, 6.7 and 32.5 Hz are assigned to C^{meta}, C^{para} and C^{ortho} carbon atoms, respectively. [17] These findingsare in agreement with the literature values. [21]

Figure 14 shows the ^{13}C-NMR spectrum of [Ph_3Sn(2-MeOPh)]. The spectrum shows only the aromatic region, as this is where most of the relevant signals are located (the entire spectrum can be found in section VII Appendix in Figure A6). There are two signals outside the range shown, a triplet at 77.16 ppm, which is a reference solvent signal of the deutero chloroform, and a further signal at 55.40 ppm, which according to the literature can be assigned to the carbon atom of the methoxy group C^7. [17]

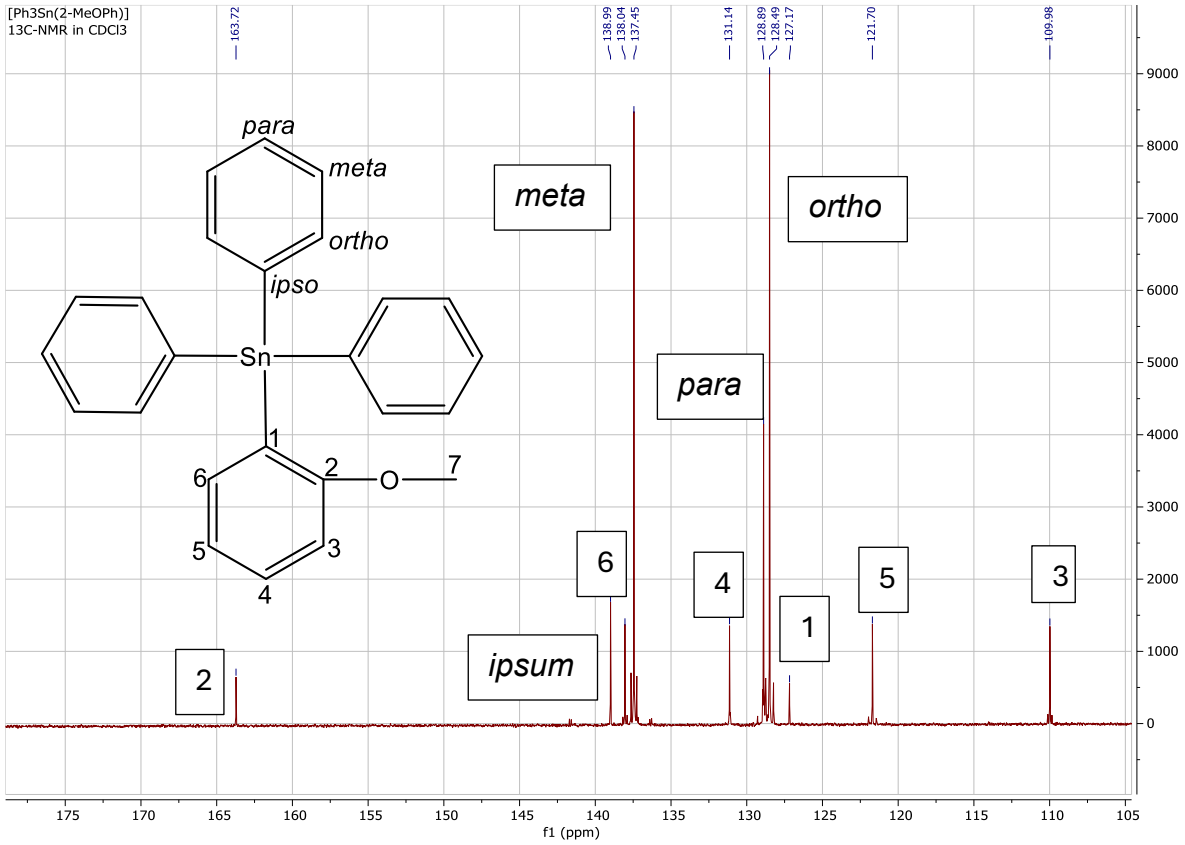

Figure 14: Illustration of the ^{13}C-NMR spectrum of [Ph_3Sn(2-MeOPh)]

According to the structure in Figure 14 the phenyl rings elicit four signal due to four carbon atoms and the 2-anisole ligand elicits six signals. One signal for each carbon atom. [17]

The signal at 138.99 ppm can be attributed to C^{ipso}, the signal at 128.49 ppm can be attributed to C^{ortho}, the signal at 137.45 ppm can be attributed to C^{meta}, the signal at 128.89 ppm can be attributed to C^{para}, the signal at 127.17 ppm can be attributed to C^1, the signal at 163.72 ppm can be attributed to C^2, the signal at 109.98 ppm can be attributed to C^3, the signal at 131.14 ppm can be attributed to C^4, the signal at 121.70 ppm can be attributed to C^5 and the signal at 138.04 ppm can be attributed to C^6.

Figure 15 is now used to analyse the ^{13}C-NMR spectrum of [Ph_3Sn(3-MeOPh)]. The sample was dissolved in deutero chloroform, producing a reference solvent signal at 77.16 ppm, as a triplet. The spectrum in Figure 15 only shows the aromatic region, as this is where most of the signals are present (the entire spectrum can be found in

section VII Appendix in Figure A9). Outside the aromatic region there is a further signal at 55.25 ppm. This signal can be assigned to the carbon atom C^7, as it lies in a typical range for methoxy groups according to the literature. [17]

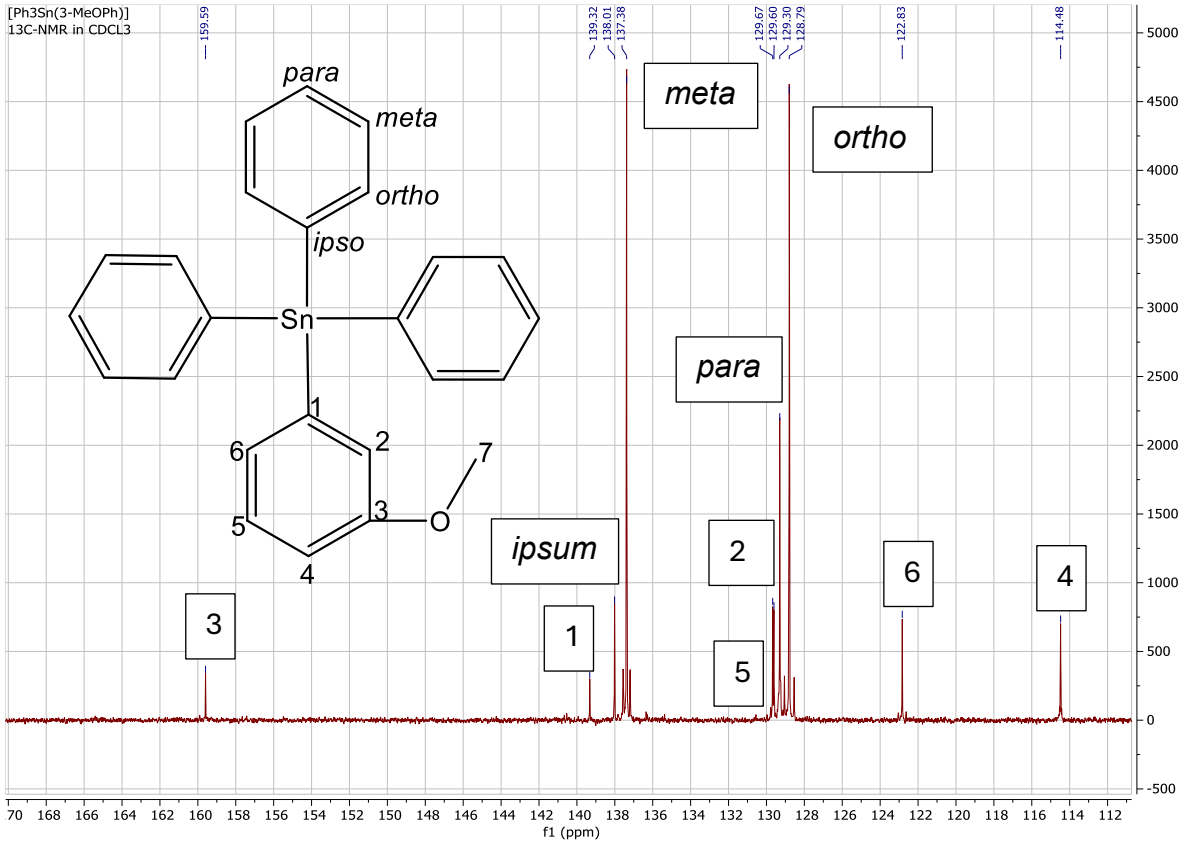

Figure 15: Illustration of the ^{13}C-NMR spectrum and the structure of [Ph_3Sn(3-MeOPh)]

The structure in Figure 15, has in addition to the already known four carbon atoms of the phenyl rings, seven further carbon atoms of the 3-anisole ligand, wich generate signals in the ^{13}C-NMR spectrum. One of these seven carbon atoms has already been assigned to the signal of the methoxy group. The other six carbon atoms are aromatically bound and therefore generate signals in the aromatic region. [17]

The signal at 138.01 ppm can be attributed to C^{ipso}, the signal at 128.79 ppm can be attributed to C^{ortho}, the signal at 137.38 ppm can be attributed to C^{meta}, the signal at 129.30 ppm can be attributed to C^{para}. The resonance at 139.32 ppm can be attributed to C^1, while the signal at 129.60 ppm can be attributed to C^2 and the signal at 159.59 ppm can be attributed to C^3. The C^4, C^5 and C^6 carbon atoms are identified at 114.48 ppm, at 129.67 ppm and at 122.83 ppm, respectively.

The ^{13}C-NMR spectrum of [Ph_3Sn(4-MeOPh)] is shown below in Figure 16. The spectrum in Figure 16 only presents the aromatic region (the entire spectrum can be found in section VII Appendix in Figure A11). Outside the aromatic region, only one signal can be recognised at 55.18 ppm, which is generated by the methoxy group and can therefore be assigned to the carbon atom C^5. This is a typical literature value for a methoxy group. [17]

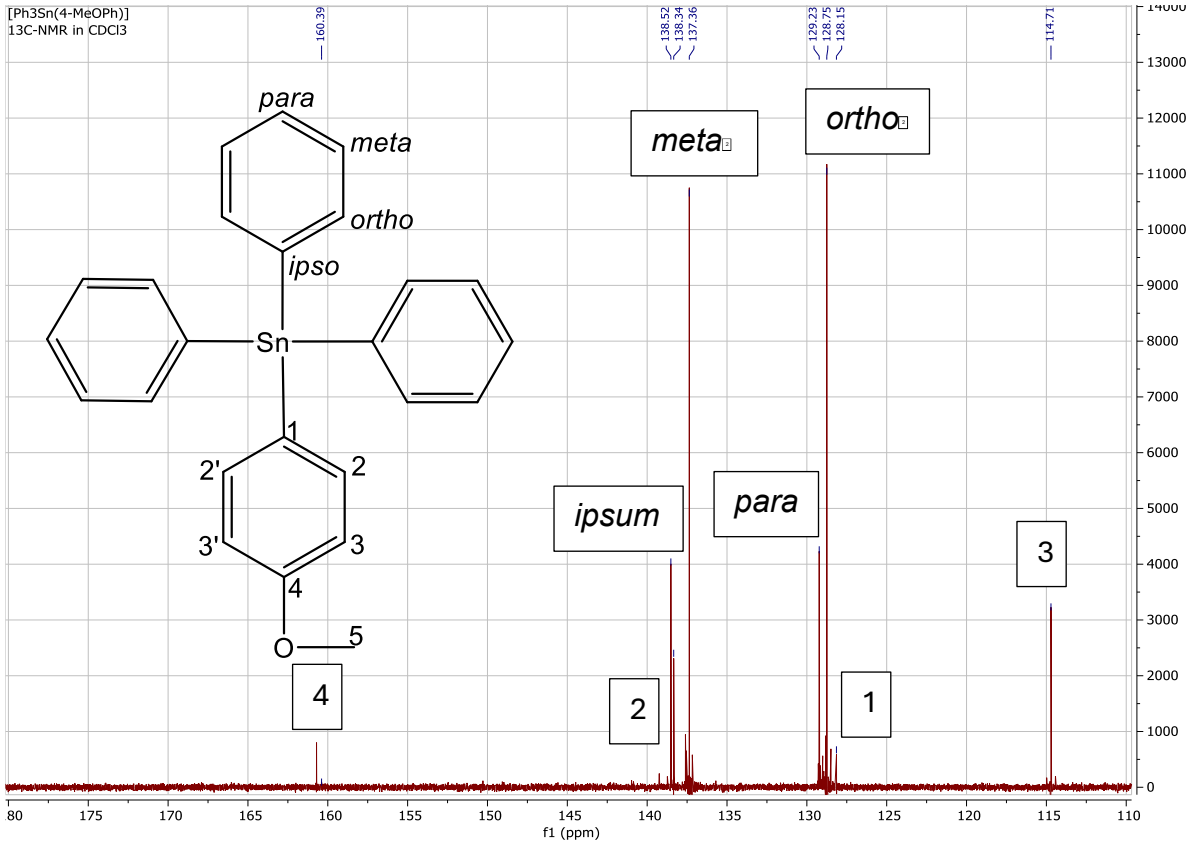

Figure 16: Illustration of the ^{13}C-NMR spectrum and the structure of [$Ph_3Sn(4\text{-}MeOPh)$]

The structure in Figure 16 shows that, in addition to the four carbon atoms typical of phenyl rings, a further five carbon atoms of the 4-anisole ligand can elicit signals in the ^{13}C-NMR spectrum. However, it should be noted that one carbon atom of the ligand has already been assigned to the methoxy group, and the four other carbon atoms are aromatically bonded. Furthermore, the carbon atoms in the C^2 and C^3 positions are chemically equivalent to the opposite carbon atoms in the C^2 and C^3 positions. As a result, only four signals are generated. [17]

The signal at 138.34 ppm can be attributed to C^{ipso}, the signal at 128.75 ppm can be attributed to C^{ortho}, the signal at 137.36 ppm can be attributed to C^{meta}, the signal at 129.23 ppm can be attributed to C^{para}. The resonance at 128.15 ppm can be attributed to C^1, while the signal at 138.52 ppm can be attributed to C^2.The C^3 and C^4 carbon atoms are identified at 114.71 ppm, at 160.39 ppm, respectively.

Due to the 2-anisole ligand, slight changes in the chemical environment also occur for the carbon atoms of the phenyl rings, which means that they cannot be assigned analogue to the TPTC. Nevertheless, the carbon atoms will give similar chemical shifts. The signals that can be assigned directly, are the signals at 137.45 ppm and 128.49 ppm, as these have the greatest intensity and can be assigned to the carbon atoms C^{meta} and C^{ortho} in analogy to the explanation for the TPTC. According to the coupling constants J of the satellite signals, for the signals with the chemical shifts at 137.45 and 128.49 ppm and the coupling constants of 19.2 and 25.2 Hz. The signal at 137.45 ppm can be assigned to the carbon atom with the label "meta"

and the signal at 128.49 ppm can be assigned to the carbon atom with the label "ortho". [17]

To be able to assign the other two carbon atoms (from the phenyl rings) to the corresponding signals, the satellite signals can be considered on the one hand and a ^{13}C-DEPT-135 NMR spectrum on the other. Whereby the quaternary carbon atoms no longer elicit a signal. In relation to the satellite signals, the signal at the chemical shift of 138.99 ppm shows very distant satellite signals. It can therefore be concluded that this signal belongs to a carbon atom that is in the immediate vicinity of a tin atom (C^{ipso}). This can also be verified by a ^{13}C-DEPT-135 NMR spectrum. Since the carbon atom C^{ipso} is not shown in the ^{13}C-DEPT-135 spectrum because it is a quaternary carbon (the ^{13}C-DEPT-135 NMR spectrum can be found in section VII Appendix in Figure A7). [17]

The ^{13}C-DEPT-135 NMR spectrum can also be used for the assignment of two carbon atoms of the 2-anisole ligand. Since this ligand has two quaternary carbon atoms, the carbon atom that binds to the tin atom (C^1) and the one that binds to the oxygen atom (C^2). The ^{13}C-DEPT-135 NMR spectrum shows that the signals 163.72 ppm and 127.17 ppm represent quaternary carbon atoms. According to the binding partners, the different mesomeric boundary structures can again be used to assign the carbon atoms to the signals. The mesomeric boundary structures for the 2-anisole ligand have already been presented for the evaluation of the ^{1}H-NMR spectrum of [Ph_3Sn(2-MeOPh)]. This showed that the carbon atoms C^1, C^3 and C^5 can each have a positive charge, which means that these carbon atoms are particularly strongly shielded. Accordingly, the carbon atom C^2 can be assigned to the signal at 163.72 ppm. In addition, this assignment can be justified by the fact that the oxygen atom, corresponding to the high electron negativity, deshields the carbon atom C^2 particularly strongly. According to these conclusions, the carbon atom C^1 can be assigned to the signal at 127.17 ppm. [17]

The last carbon atom of the phenyl rings, C^{para}, can now be assigned to two different signals, the signal at 131.14 ppm and at 128.89 ppm. In order to make an exact assignment, it is advisable to carry out an H,C-COSY-NMR measurement of the sample. The ^{1}H-NMR spectrum can be used to assign the carbon atom to a signal more easily. Since the carbon atom C^{para} is a carbon atom in the para position, the carbon atom must cause a signal at the chemical shift of the triplet at 7.40 ppm according to the evaluation of the ^{1}H-NMR spectrum. Figure 17 below shows the corresponding H,C-COSY-NMR spectrum of [Ph_3Sn(2-MeOPh)]. This spectrum can also be used to assign the carbon atoms C^3, C^4, $C^5$and C^6 to a signal. [17]

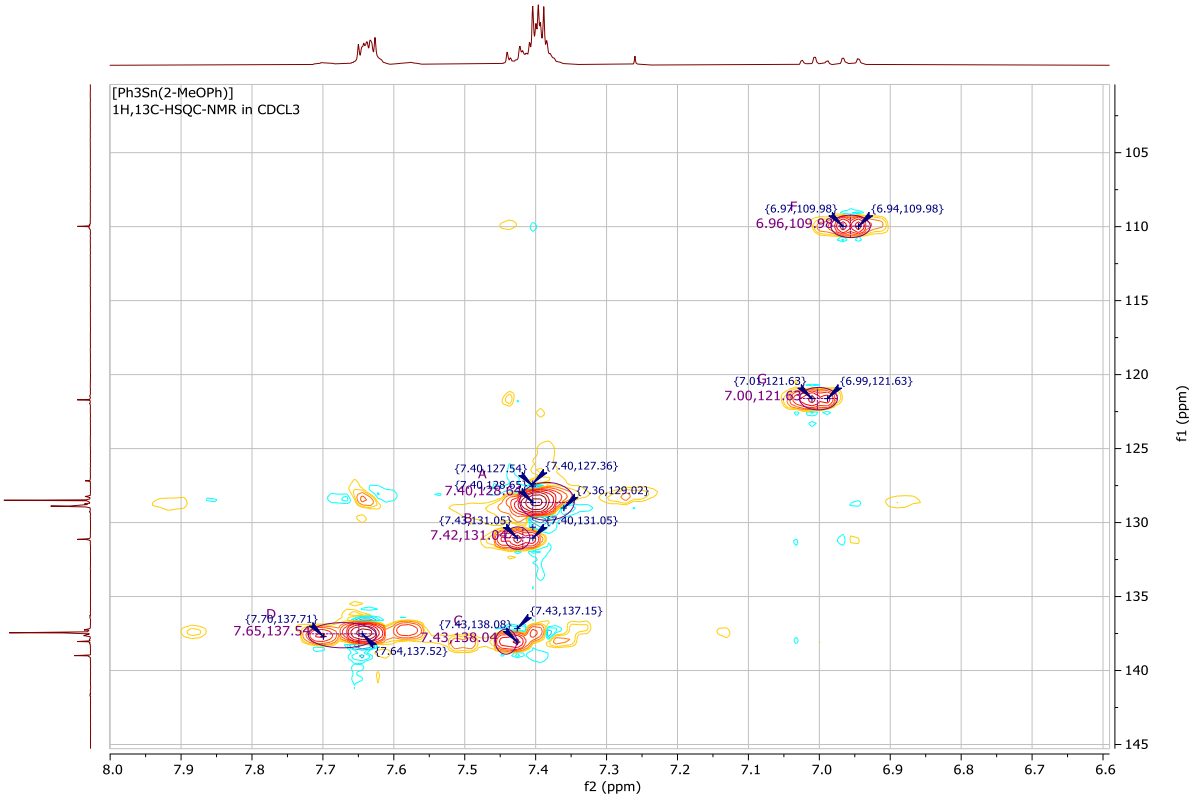

Figure 17: Illustration of the C,H-COSY-NMR spectrum of [Ph_3Sn(2-MeOPh)]

According to the H,C-COSY-NMR spectrum from Figure 17, it can be recognised that the carbon signal at 128.89 ppm binds to a hydrogen atom that can be assigned to the triplet at 7.40 ppm. Consequently, the carbon atom C^{para} can be assigned to the signal of the ^{13}C-NMR spectrum at 128.89 ppm. [17]

The carbon atom C^6 is bonded to the hydrogen atom assigned to the duplet at 7.44 ppm. When looking at the H,C-COSY-NMR spectrum from Figure 17, the duplet at 7.44 ppm can be assigned to the signal at 131.62 ppm of the ^{13}C-NMR spectrum. Therefore, it justifies that the carbon atom C^6 can be assigned to the signal at 131.62 ppm. In addition to that, this can be justified based on the mesomeric boundary structures. Since the carbon atom C^6 has no positive charge and is therefore more strongly deshielded compared to the carbon atoms C^1, C^3 and C^5. [17]

Regarding the carbon atom C^5, it is strongly shielded according to the mesomeric boundary structures and binds to the hydrogen atom that causes the triplet at 7.01 ppm. According to the spectrum in Figure 17, this hydrogen atom binds to a carbon atom, which produces a signal at 121.70 ppm. Therefore the carbon atom C^5 can be assigned to the signal of the ^{13}C-NMR spectrum at 121.70 ppm. [17]

The carbon atom C^4, on the other hand, has no positive charge, corresponding to the mesomeric boundary structures, which means that it is more strongly shielded. However, this carbon atom binds to a hydrogen atom, which elicit a triplet at 7.42 ppm.

By observing the spectrum in Figure 14, this hydrogen atom binds to a carbon atom that produces a signal at 131.14 ppm. Consequently, the carbon atom C^4 can be assigned to the ^{13}C-NMR signal at 131.14 ppm. [17]

Finally, the carbon atom C^3 can be assigned, whereby it must be noted that this carbon atom is strongly shielded according to the mesomeric boundary structures and at the same time binds to a hydrogen atom, which produces a doublet at 6.96 ppm. Consequently, it can be seen from the spectrum in Figure 17 that this hydrogen atom binds to a carbon atom that produces a signal at 109.98 ppm. As a result, the carbon atom C^3 can be assigned to the ^{13}C-NMR signal at 109.98 ppm. [17]

In conclusion, it can be stated for [Ph_3Sn(2-MeOPh)] that all carbon atoms could be successfully assigned.

The signals of the carbon atoms of the phenyl rings show, similar chemical shifts compared to [Ph_3Sn(2-MeOPh)]. This is due to the influence of the 3-anisole ligand. However, as there are only small differences, it can be concluded that the signals at 138.01 ppm, 137.38 ppm, 129.30 ppm and 128.79 ppm can be assigned to the carbon atoms of the phenyl rings. Including the reasoning with the satellite signals, these signals can be assigned directly to the carbon atoms. The signal at 138.01 ppm has satellite signals with the largest coupling constant of 264.7 Hz, while the signal at 128.79 ppm has the second largest coupling constant of 25.9 Hz (in relation to the satellite signals). In contrast to that, the signal at 137.38 ppm has satellite signals with a coupling constant of 18.9 Hz, which is the second smallest coupling constant, and the signal at 129.30 ppm has the smallest coupling constant at 3.2 Hz (in relation to the satellite signals). Considering that the coupling constant becomes smaller the further away the carbon atom is from the tin atom, the carbon atom labelled "*ipsum*" can be assigned to the signal at 138.01 ppm, the carbon atom labelled "*ortho*" to the signal at 128.79 ppm, the carbon atom labelled "*meta*" to the signal at 137.38 ppm and the carbon atom labelled "*para*" to the signal at 129.30 ppm. [17]

To be able to assign the carbon atoms of the 3-anisole ligand, a ^{13}C-DEPT-135 spectrum can be recorded (this spectrum can be found in section VII Appendix in Figure A10). This shows that the signals at 159.59 ppm, 139.32 ppm and 138.01 ppm are caused by quaternary carbon atoms. This also supports the assignment of the carbon atom labelled "*ipsum*" to the signal at 138.01 ppm. The two signals at 159.59 ppm and 139.32 ppm therefore belong to the carbon atoms of the 3-anisole ligand. This also overlaps with the structure of the ligand, as it only has two quaternary carbon atoms. These are the carbon atom that binds to the tin atom (C^1) and the carbon atom that binds to the oxygen atom (C^3). These can be assigned solely by the differences in the electron negativities of the carbon atoms, the tin atom and the oxygen atom. The carbon atom C^3 is strongly deshielded by the high electron negativity of the oxygen atom, as it has a large electron cloud. As a result, it can be assigned to the signal at 159.59 ppm. The carbon atom C^1 is not significantly shielded by the tin atom, as the carbon atom has a higher electron negativity than the tin atom. As a result, the carbon atom C^1can be assigned to the signal at 139.32 ppm. [17]

To be able to assign the carbon atom C^5, the mesomeric boundary structures can be used again. This shows that the carbon atom in question has no positive charge and is therefore deshielded. It should also be noted that the other carbon atoms that have not yet been assigned can all have a positive charge and are therefore more strongly shielded. This means that the carbon atom C^5 can be assigned to the signal at 129.67 ppm. [17]

An H,C-COSY-NMR spectrum can be used for the as yet unassigned carbon atoms labelled C^2, C^4 and C^6. It is only important to know to which hydrogen atoms the carbon atoms bind or to which chemical shifts the hydrogen atoms generate signals. The H,C-COSY-NMR spectrum is shown below in Figure 18 (however, the H,C-COSY-NMR spectrum may have slightly different chemical shifts in the 0.01 ppm range).

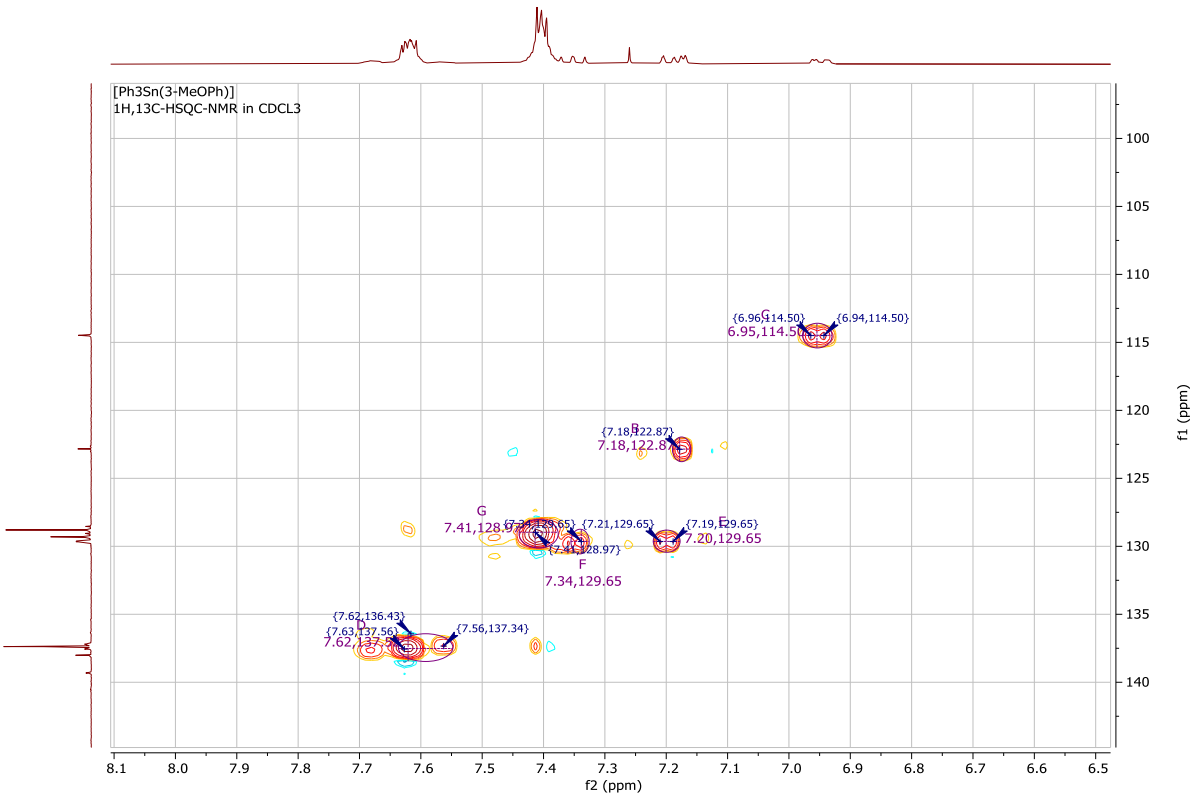

Figure 18: Illustration of the H,C-COSY-NMR spectrum of [Ph_3Sn(3-MeOPh)]

Considering that the hydrogen atom that binds to the carbon atom C^4 produces a doublet at 6.95 ppm. This carbon atom can be assigned to the ^{13}C-NMR signal at 114.48 ppm. This interpretation also overlaps with the statement from section "2.2.1 Analysis of the ^{1}H-NMR spectra" where the carbon atom mentioned is the most shielded carbon atom. [17]

In contrast to that, the carbon atom C^6 binds to a hydrogen atom, which produces a doublet at 7.18 ppm. Allowing this carbon atom to be assigned to the ^{13}C-NMR signal at 112.83 ppm. This overlaps with the interpretation that it is deshielded by the slightly increased electron density of the carbon atom C^1, compared to the carbon atom C^4. [17]

The carbon atom C^2 binds directly to a hydrogen atom, which generates a singlet at 7.20 ppm and can therefore be assigned to the ^{13}C-NMR signal at 129.60 ppm. This conclusion overlaps with the interpretation from section "2.2.1 Analysis of the ^{1}H-NMR spectra". [17]

Thus, all carbon atoms of the triphenyl(3-anisole)tin(IV) complex were successfully assigned to signals, confirming the success of the synthesis.

As already explained for the other samples, there is a small deviation in the chemical shifts for the carbon atoms of the phenyl rings compared to the TPTC. Nevertheless, three of the four carbon atoms can be directly assigned to signals. This assignment is mainly due to the satellite signals and the similar intensities compared to the TPTC. Here, the satellite signals of the signal at 129.23 ppm have a coupling constant of 5.6 Hz. In contrast, the coupling constant for the satellite signals of the signal at 137.36 ppm is 18.9 Hz. For the signal at 128.75 ppm, the coupling constant of the satellite signals is 25.7 Hz. Considering that the coupling constant decreases with the distance to the tin atom, the carbon atom labelled "*ortho*" can be assigned to the signal at 128.75 ppm. Furthermore, the signal at 137.36 ppm can be assigned to the carbon atom labelled "*meta*" and the signal at 129.23 ppm can be assigned to the carbon atom labelled "*para*". [17]

The fourth signal, which cannot be directly assigned to the phenyl rings, is the signal for the carbon atom labelled "*ipsum*", which would have the largest coupling constant. However, as there are only slight deviations in the chemical shifts compared to the TPTC, the carbon atom must be assigned to one of the two signals at 138.52 ppm or 138.34 ppm. This assignment can be made by recording a ^{13}C-DEPT-135 NMR spectrum (this spectrum can be found in section VII Appendix in Figure A13). In this spectrum, the signal at 138.34 ppm is no longer displayed, as this is a quaternary carbon atom. This signal can therefore be assigned to the carbon atom labelled "ipsum". Furthermore, the coupling constant of the satellite signals of 264.8 Hz shows that this signal has the largest coupling constant. [17]

In addition, it can be seen from the ^{13}C-DEPT-135 NMR spectrum that the signals at 160.39 ppm and 128.15 ppm are also quaternary carbon atoms. According to the structure in Figure 16, these signals can only be assigned to the carbon atoms C^1 and C^4. The carbon atom C^4 is strongly deshielded by the methoxy group and can therefore be assigned to the signal at 160.39 ppm. In contrast, the carbon atom C^1 is not particularly shielded by the tin atom. Furthermore, considering the mesomeric boundary structures of the 4-anisole ligand, a positive charge may be present on this carbon atom, which shields this carbon atom. Thus, the carbon atom C^1 can be clearly assigned to the signal at 128.15 ppm. [17]

The carbon atoms C^2 and C^3 can only be assigned to the signals at 138.52 ppm and 114.71 ppm. The mesomeric boundary structures of the 4-anisole ligand can be considered again for this assignment. A positive charge can be present at the carbon atom C^3 and that no positive charge can be present at the carbon atom C^2. As a result, the carbon atom C^3 can be assigned to the signal at 114.71 ppm, as it is more strongly

shielded by the positive charge. In contrast, the carbon atom C^2 can be assigned to the signal at 138.52 ppm. [17]

In conclusion, it can be stated that all carbon atoms of [Ph_3Sn(4-MeOPh)] could be successfully assigned to the complex triphenyl(4-anisole)tin(IV). Consequently, the synthesis was successful. Furthermore, no additional signals due to impurities can be recognised in the ^{13}C-NMR spectrum.

2.2.3 Analysis of the ^{119}Sn-NMR spectra

In this section, the results of the ^{119}Sn-NMR spectra of [Ph_3Sn(*n*-MeOPh)] (*n* = 2–4) are presented and analysed (the ^{119}Sn-NMR spectra can be found in section VII Appendix in Figure A14 to Figure A17).

For the [Ph_3Sn(2-MeOPh)] there is only one signal in the ^{119}Sn-NMR spectrum, which is at -125.77 ppm. This chemical shift shows a strong difference to the chemical shift of the starting compound TPTC, which has a resonance in ^{119}Sn NMR spectrum at -45.24 ppm. It can therefore be concluded that the reactant TPTC is no longer present in the sample, by the sensitivity of ^{119}Sn NMR spectroscopy, and only the desired product detected.

There is also only one resonance found in the ^{119}Sn-NMR spectrum for [Ph_3Sn(3-MeOPh)] or [Ph_4Sn(4-MeOPh)] at -128.41 or -125.89 ppm, respectively. According to a comparison with the resonance of the TPTC it can be concluded that both compounds were also successfully prepared. This interpretation is additionally supported by the fact that ^{119}Sn-NMR chemicals shifts of samples [Ph_3Sn(*n*-MeOPh)] (*n* = 2–4) should not differ significantly from each other, as they have similar chemical structures.

The signals of all complexes are in a range which is typical for tin(IV) complexes with coordination number 4 with tetrahedral arrangement around tin atom. Furthermore, the determined chemical shifts are very close to the chemical shift of tetrakis(phenyl)tin(IV), which supports the presented interpretations. [20]

2.2.4 Evaluation of the IR-spectra

In this section, the results of the infrared spectroscopy are presented and analysed. The samples are analysed in the order [Ph_3Sn(2-MeOPh)], [Ph_3Sn(3-MeOPh)] and [Ph_3Sn(4-MeOPh)], correspondingly from the 2-anisole sample to the 3-anisole sample up to the 4-anisole sample.

Figure 19 shows the infrared spectrum of [Ph_3Sn(2-MeOPh)]. Characteristic bands have also been labelled in this spectrum.

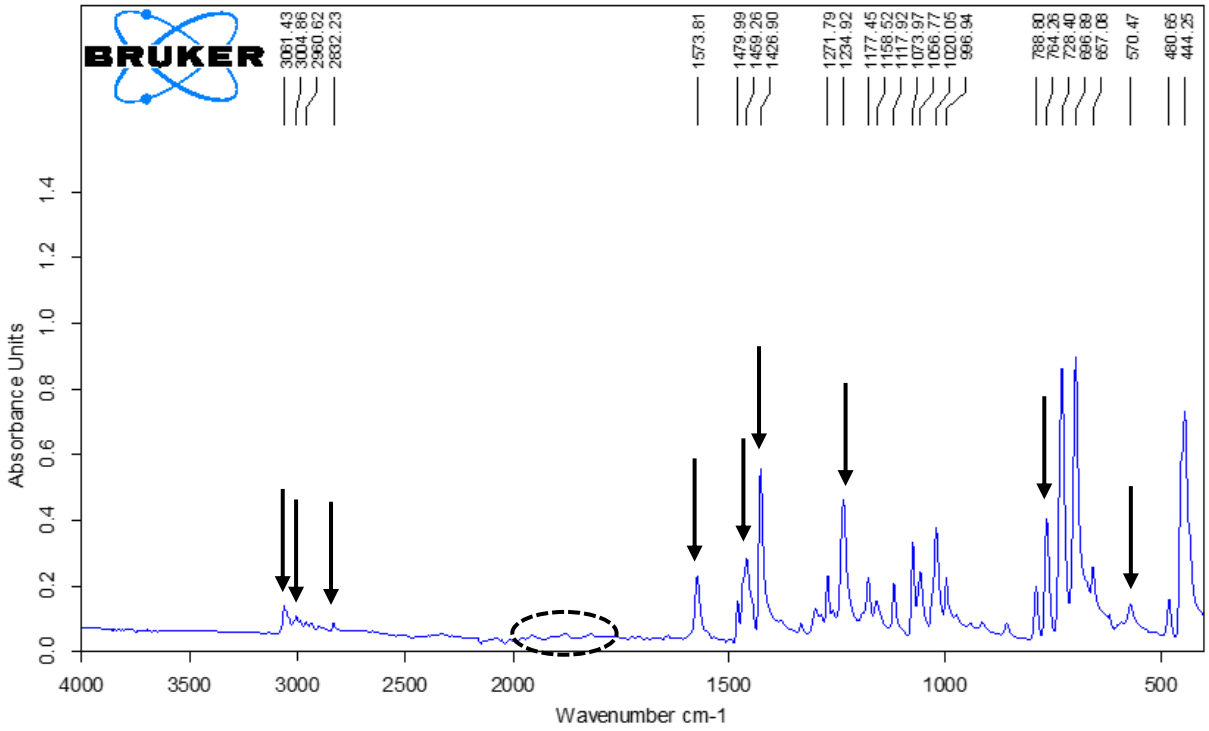

Figure 19: IR-spectrum of [$Ph_3Sn(2\text{-}MeOPh)$]

As shown in Figure 19, [$Ph_3Sn(2\text{-}MeOPh)$] has nine characteristic bands. Three bands can be recognised in the range from 2832.23 to 3061.43 cm^{-1}. The band at 3061.43 cm^{-1}can be assigned to the valence vibrations of the aromatically bonded hydrogen atoms. The band at 3004.86 cm^{-1}, on the other hand, represents the valence vibration of a methyl group. Whereas the band at 2832.23 cm^{-1}represents the valence vibration of a methoxy group (this methyl or methoxy group can be assigned to the ligand 2-anisole). In addition to the band at 3061.43 cm^{-1}, the valence vibration of the aromatic ring can also be recognised by the bands at 1573.81, 1459.26 and 1426.90 cm^{-1}. In addition, so-called "benzene fingers" [22], which are typical for an aromatic system, can be recognised in the range from 1700 to 2000 cm^{-1}. Furthermore, due to the methoxy group present, an ether group can be recognised by the band at 1271.79 cm^{-1}. In addition to confirming that it is an anisole ligand, the band at 788.80 cm^{-1} can be used to recognise that it is an *ortho*-substituted ligand. The band at 788.80 cm^{-1} represents an out-of-plane vibrational mode. The characteristic Sn–C bonds can be recognised mainly in the band at 570.47 cm^{-1}. The band at 570.47 cm^{-1} represents the binding of the tin atom to the ligand, 2-anisole. [17,23]

To further visualise the conversion of triphenyltin(IV) chloride to triphenyl(2-anisole)tin(IV), the infrared spectrum of [$Ph_3Sn(2\text{-}MeOPh)$] can be compared with that of TPTC (see section VII Appendix for an IR spectrum in which both samples were superimposed and the differences were marked).

The first difference can be recognised in the range from 2832.23 to 3004.86 cm^{-1}. This is since [$Ph_3Sn(2\text{-}MeOPh)$] has a methyl or methoxy group and therefore represents characteristic vibrations. Due to the absence of the methyl or methoxy

group, TPTC also does not exhibit a vibration in the range of 1271.79 cm^{-1}, whereby this can be assigned to an ether group as mentioned. Furthermore, TPTC has one band less in the range from 1426.90 to 1573.81 cm^{-1}. This is because of TPTC has a less pronounced aromatic system than [Ph_3Sn(2-MeOPh)], as TPTC only has three aromatic substituents and not four like [Ph_3Sn(2-MeOPh)]. In addition, the substitution with the ligand can be explained by the band at 788.80 cm^{-1}. Since TPTC does not has this band, as there is no *ortho*-substituted derivative. In addition to that, the TPTC has no band at 570.47 cm^{-1}. Whereby this is due to the binding of the 2-anisole ligand, which is not present in TPTC.

According to the previous findings, it can be concluded that the synthesis for [Ph_3Sn(2-MeOPh)] was successful, and the desired product could be synthesised.

Figure 20 shows the IR spectrum of [Ph_3Sn(3-MeOPh)]. The characteristic bands are emphasised.

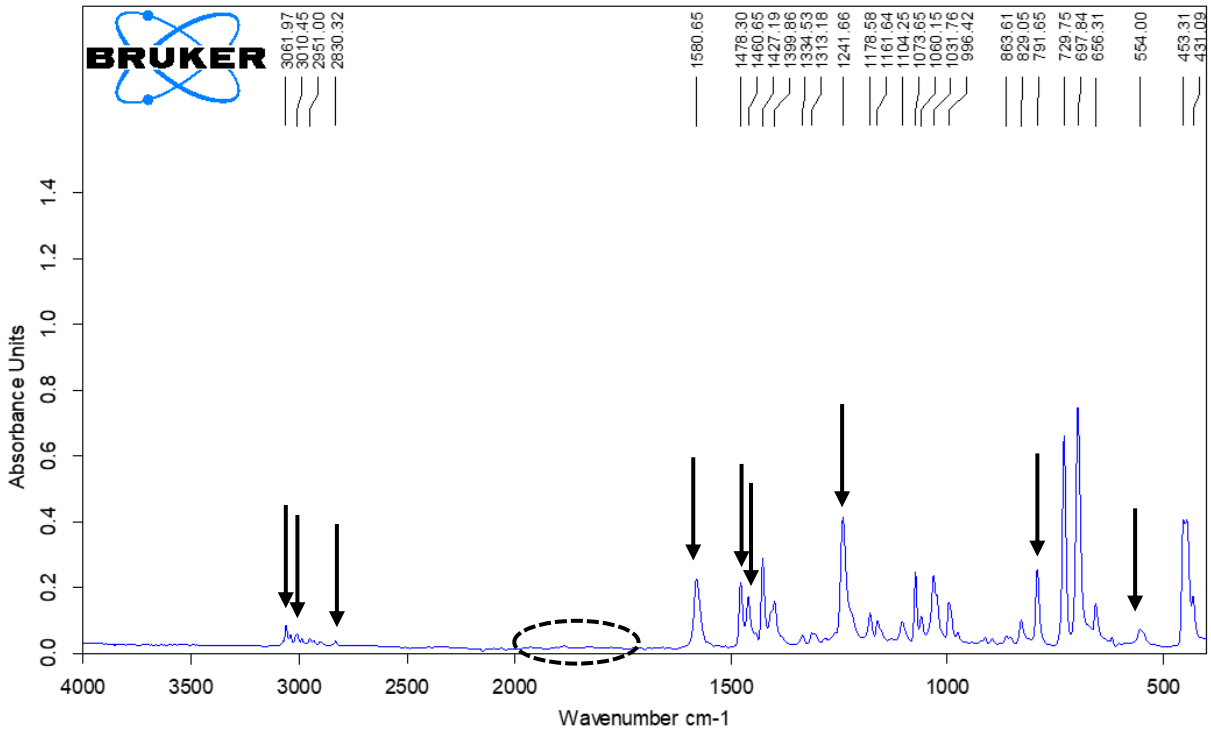

Figure 20: Representation of the IR spectrum for [Ph_3Sn(3-MeOPh)]

As can be seen in Figure 20, [Ph_3Sn(3-MeOPh)] differs only slightly from [Ph_3Sn(2-MeOPh)] according to its bands, with mainly slight deviations in the wave number for the characteristic bands, such as the valence vibration of the aromatically bonded hydrogen atoms, the valence vibration of the methyl residue or the methoxy group, the valence vibration of the aromatic ring, as well as the so-called "benzene fingers" [22], the ether group and the stretching vibration of the tin-aryl bond. The main change lies in the characteristic band for the *meta*-substituted derivatives, which can be recognised by the band at 791.65 cm^{-1}. This shows the presence of the 3-anisole ligand. Furthermore, there is another band at 554 cm^{-1}, which can be assigned to the Sn–C bond or the stretching vibration of this bond. [17,23]

The infrared spectrum of [Ph_3Sn(3-MeOPh)] can also be compared with the infrared spectrum of TPTC to illustrate the success of the synthesis (an IR spectrum can be taken from section VII Appendix, in which both samples were superimposed, and the differences were marked).

Figure 21 shows the IR spectrum of [Ph_3Sn(4-MeOPh)]. The characteristic bands are again emphasised with arrows and dotted ellipsoid.

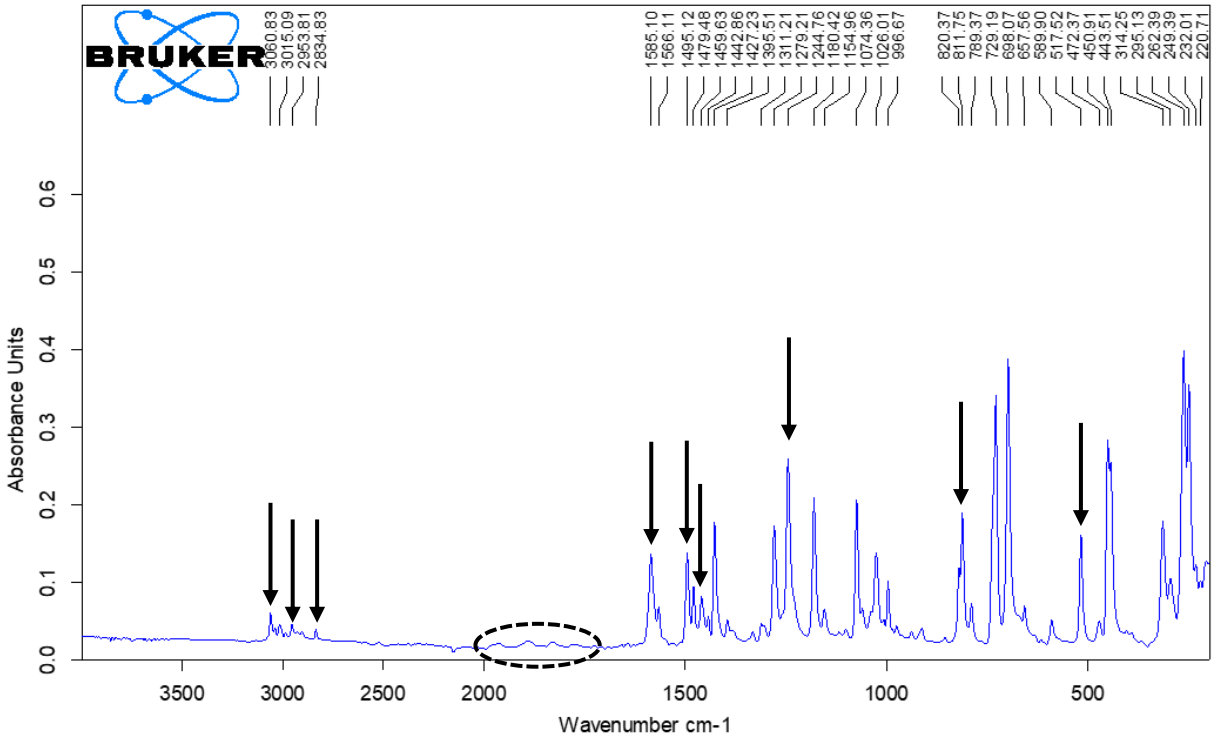

Figure 21: Illustration of the IR spectrum for [Ph_3Sn(4-MeOPh)]

Similar to [Ph_3Sn(2-MeOPh)] and [Ph_3Sn(3-MeOPh)], the IR spectrum of [Ph_3Sn(4-MeOPh)] (Figure 21) shows characteristic bands for the valence vibration of the aromatically bonded H atoms, the methyl and methoxy groups and the aromatic system. Furthermore, the bands for the "benzene fingers" [22], the ether group and a band for the Sn–C bond or its stretching vibration can be recognised in a comparable range in relation to [Ph_3Sn(3-MeOPh)] [23]. The biggest difference is again in the band which describes the substitution pattern. [Ph_3Sn(4-MeOPh)] exhibits a *para*-substituted derivative, which is represented in the IR spectrum by the band at 811.75 cm^{-1}. [17]

As already shown for [Ph_3Sn(2-MeOPh)] and [Ph_3Sn(3-MeOPh)], it can also be recognised for [Ph_3Sn(4-MeOPh)] that TPTC does not have characteristic bands that [Ph_3Sn(4-MeOPh)] has.

3. Conclusion

Due to the flexible properties of organotin compounds in relation to possible substitution patterns and the associated different applications in anticancer therapy, these compounds have proven to be excellent candidates in the fight against malignant cells. Because of that the interest in research in this area has increased significantly over the last few decades, as evidenced by the large number of published studies.

In the field of organotin compounds, triphenyltin(IV) compounds have established themselves as particularly promising candidates in the fight against malignant cells, whereby this is due to the strong biological activity of these compounds. It is therefore of interest to further investigate and optimise the synthesis of such triphenyltin(IV) compounds.

In this context, the aim of this work was to develop a new synthetic route to synthesise some known compounds that had not yet been characterised, to synthesise a completely new compound and to fully characterise all synthesised compounds.

Three compounds were synthesised: [Ph_3Sn(2-MeOPh)], [Ph_3Sn(3-MeOPh)] and [Ph_3Sn(4-MeOPh)], triphenyl(2-/3-/4-anisole)tin(IV) complexes. The [Ph_3Sn(*n*-MeOPh)] (*n* = 2–4)were obtained in a yield of 44.7, 73.0 and 88.5%, respectively. This distribution of the yields can also be attributed to the steric hindrance of the individual complexes. Since the complex [Ph_3Sn(4-MeOPh)] is the least sterically hindered due to the MeO group in *para* position of 4-anisole ligand. On the other side [Ph_3Sn(2-MeOPh)] as the most sterically hindered due to the MeO group in the *ortho* position. Therefore, it can be concluded that steric hindrance is directly related to the yield of the complexes.

All synthesised complexes were also investigated spectroscopically using multinuclear (^{1}H-, ^{13}C- and ^{119}Sn) NMR and IR spectroscopy. The structure was elucidated in certain cases, using a ^{13}C-DEPT-135 and an H,C-COSY NMR spectra. Thus, all three complexes could be successfully prepared. Furthermore, all complexes were analysed for their purity by means of elemental analysis, which showed that all three can be classified as highly pure.

4. Experimental Part

4.1 Materials and Methods

A Schlenk technique was used for the synthesis of [Ph_3Sn(2-MeOPh)], [Ph_3Sn(3-MeOPh)] and [Ph_3Sn(4-MeOPh)], whereby the reactions were carried out under a nitrogen atmosphere. The materials were used as purchased and not further pretreated. The chemicals used were magnesium (99%, TCI), iodine (99.5%, Roth), 2-bromoanisole (98%, Thermo Fisher Scientific), 3-bromoanisole (99%, Thermo Fisher Scientific), 4-bromoanisole (99%, Sigma-Aldrich), diethyl ether (99.5%, Roth), triphenyltin chloride (95%, Carl Roth), methanol (ROTISOLV HPLC grade, Carl Roth) and n-hexane (99%, Carl Roth).

The synthesised complexes were characterised using multinuclear NMR spectroscopy in the form of ^{1}H-, ^{13}C-, ^{13}C-DEPT-135-, H,C-COSY- and ^{119}Sn NMR. The synthesis and all characterizations were performed at the University of Applied Sciences Merseburg. The NMR spectroscopy was performed using a Bruker AVANCE DRX 400 NMR spectrometer. Deutero chloroform ($CDCl_3$) was used as the solvent for all NMR samples. For the ^{1}H (400 MHz) and ^{13}C (101 MHz) spectra, tetramethylsilane was used as the internal standard. Elemental analysis was performed using a Thermo Scientific FlashSmart CHNS instrument. Infrared spectroscopy was performed using a BRUKER VERTEX70 device with a BRUKER PLATINUM ATR unit.

4.2 Synthesis of the Complexes

In this section, the syntheses of the individual complexes are presented together with the analytical results and the yields.

4.2.1 Synthesis of triphenyl(2-anisole)tin(IV)

For the synthesis of the triphenyl(2-anisole)tin(IV) complex, the synthesis route described in section "2.1 Synthesis of the compounds" is used. Accordingly, 0.4 g of magnesium, a small amount of iodine and 1.5 mL of 2-bromoanisole, which is first dissolved in 30 mL of diethyl ether, are added to a round bottom flask. The 2-bromoanisole solution is then added slowly over a period of 1 h. The solution is then boiled under reflux for 2 h and cooled with an ice bath after boiling. At the same time, 2.02 g triphenyltin chloride is pre-dissolved in 40 mL diethyl ether, which is then added slowly over 15 min. This solution is then boiled again for 2 h under reflux and, after the

boiling process, cooled to room temperature and stirred. The reaction is then quenched with 10 mL of a 1 M hydrochloric acid solution, which is added slowly. The resulting aqueous phase is separated and washed three times with 10 mL diethyl ether each time, whereupon all organic phases are combined and dried with 10 spoonful of magnesium sulphate, which is then filtered off. The solvent is evaporated from the dry solution and the resulting white product is washed successively with 10 mL methanol and 10 mL *n*-hexane.

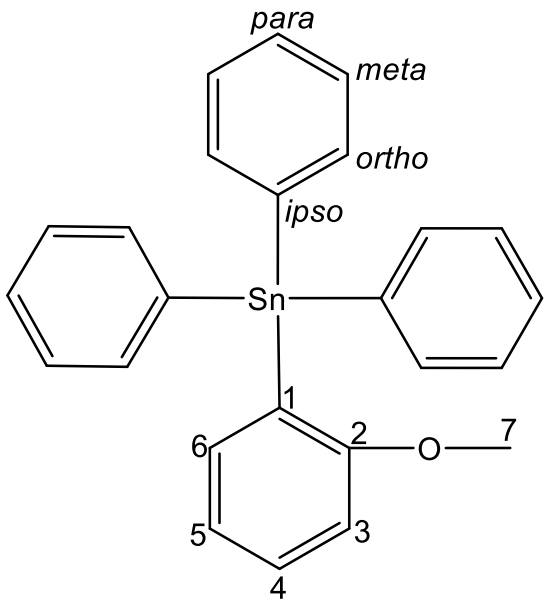

Figure 22: Structure of triphenyl(2-anisole)tin(IV)

White-solid, $C_{25}H_{22}OSn$, Mr = 457.16 g*mol^{-1}

Yield = 1.07 g (44.7%)

^{1}H NMR (400 MHz, *CDCl$_3$*) δ [ppm]:
7.64 (m, 1H; C^{ortho} *H*), 7.44 (d, *J* = 1.8 Hz, 1H; C^{6} *H*), 7.42 (d, *J* = 1.5 Hz, 1H; C^{4} *H*), 7.40 (m, 9H; C^{meta} *H*, C^{para} *H*), 7.01 (t, *J* = 7.2 Hz, 1H; C^{5} *H*), 6.96 (d, *J* = 8.6 Hz, 1H; C^{3} *H*), 3.75 (s, 3H; C^{7} *H*).

^{13}C NMR (101 MHz, *CDCl$_3$*) δ [ppm]:
163.72 (C^{2}), 138.99 (C^{ipsum}), 138.04 (C^{6}), 137.45 (C^{meta}), 131.14 (C^{4}), 128.89 (C^{para}), 128.49 (C^{ortho}), 127.17 (C^{1}), 121.70 (C^{5}), 109.98 (C^{3}), 55.40 (C^{7}).

^{119}Sn NMR (149 MHz, *CDCl$_3$*) δ [ppm]:
-125.77.

IR $\tilde{\nu}$ [cm^{-1}]:
3061.43 (aryl-H), 3004.86 (CH_3), 2832.23 (OCH_3), 1573.81, 1459.26, 1426.90 (aryl-H), 1271.79 (C-O-C), 788.80 (1,2-disubstituation), 570.47 (Sn-C)

Elemental analysis: calculated (%) for $C_{25}H_{22}OSn$: C, 65.68; H, 4.85; found: C, 65.37; H, 4.81

4.2.2 Synthesis of triphenyl(3-anisole)tin(IV)

The complex triphenyl(3-anisole)tin(IV) is synthesised in the same way as described in section "4.2.1 Synthesis of Triphenyl(2-anisole)tin(IV)", whereby slightly different masses are used for the magnesium and triphenyltin chloride. The ligand 3-bromoanisole is used instead of the 2-bromoanisole. In this case, 0.41 g magnesium

is used and 2.02 g triphenyltin chloride is used. In addition, the triphenyltin chloride was pre-dissolved in 45 mL diethyl ether.

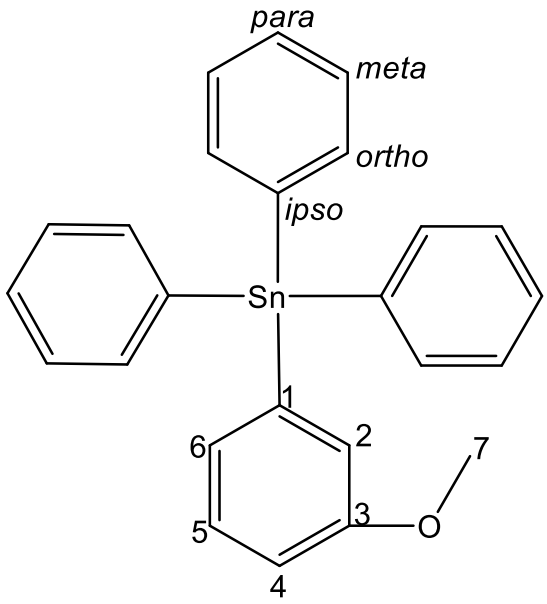

Figure 23: Structure of triphenyl(3-anisole)tin(IV)

White-solid, $C_{25}H_{22}OSn$, Mr = 457.16 g*mol^{-1}

Yield = 1.75 g (73.0%)

^{1}H NMR (400 MHz, *CDCl$_3$*) δ [ppm]:
7.62 (m, 6H, C^{ortho} *H*), 7.40 (m, 9H, C^{meta} *H*, C^{para} *H*), 7.35 (t, 1H, C^{5} *H*), 7.19 (s, 1H, C^{2} *H*), 7.17 (d, *J* = 2.8 Hz, 1H, C^{6} *H*), 6.94 (ddd, *J* = 8.3, 2.8, 1.0 Hz, 1H, C^{4} *H*), 3.78 (s, 3H, C^{7} *H*).

^{13}C NMR (101 MHz, *CDCl$_3$*) δ [ppm]:
159.59 (C^{3}), 129.32 (C^{1}), 138.01 (C^{ipsum}), 137.38 (C^{meta}), 129.67 (C^{5}), 129.60 (C^{2}), 129.30 (C^{para}), 128.79 (C^{ortho}), 122.83 (C^{6}), 114.48 (C^{4}), 55.25 (C^{7}).

^{119}Sn NMR (149 MHz, *CDCl$_3$*) δ [ppm]:
-128.41.

IR $\tilde{\nu}$ [cm^{-1}]:
3061.97 (aryl-H), 3010.45 (CH_3), 2830.32 (OCH_3), 1580.65, 1478.30, 1460.65 (aryl-H), 1241.66 (C-O-C), 791.65 (1,3-disubstituation), 554.00 (Sn-C)

Elemental analysis: calculated (%) for $C_{25}H_{22}OSn$: C, 65.68; H, 4.85;
found: C, 65.34; H, 4.82

4.2.3 Synthesis of triphenyl(4-anisole)tin(IV)

The triphenyl(4-anisole)tin(IV) complex is also synthesised analogously to the synthesis route described in section "4.2.1 Synthesis of triphenyl(2-anisole)tin(IV)". Here, 0.4 g of magnesium was added to the flask together with a small crumb of iodine. The ligand used was 4-bromoanisole, but 1.5 mL of this was also dissolved in 30 mL diethyl ether. In relation to triphenyltin chloride, 2 g were dissolved in 40 mL diethyl ether.

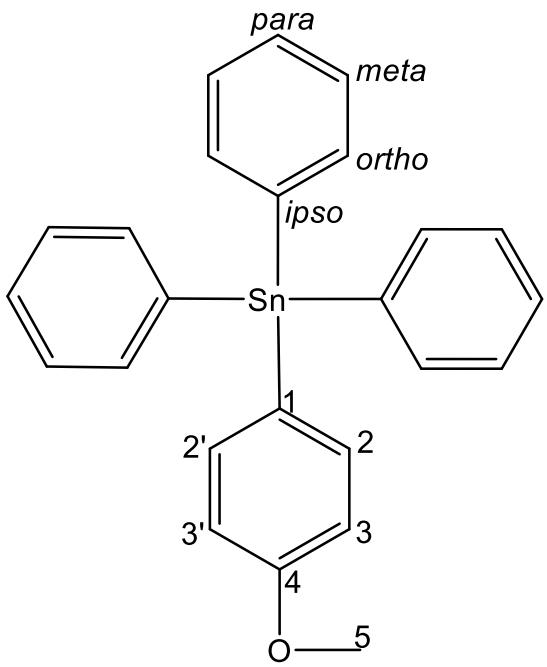

Figure 24: Structure of triphenyl(4-anisole)tin(IV)

White-solid, $C_{25}H_{22}OSn$, Mr = 457.16 g*mol^{-1}

Yield = 2.1 g (88.5%)

^{1}H NMR (400 MHz, *CDCl$_3$*) δ [ppm]:
7.61 (m, 6H; $C^{ortho}H$), 7.52 (d, *J* = 8.6 Hz, 2H; $C^{2}H$), 7.40 (m, 9H; $C^{meta}H$; $C^{para}H$), 6.97 (d, *J* = 8.6 Hz, 2H; $C^{3}H$), 3.82 (s, 3H; $C^{5}H$).

^{13}C NMR (101 MHz, *CDCl$_3$*) δ [ppm]:
160.39 (C^{4}), 138.52 (C^{2}), 138.34 (C^{ipsum}), 137.36 (C^{meta}), 129.23 (C^{para}), 128.75 (C^{ortho}), 128.15 (C^{1}), 114.71 (C^{3}), 55.18 (C^{5}).

^{119}Sn NMR (149 MHz, *CDCl$_3$*) δ [ppm]:
-125.89.

IR $\tilde{\nu}$ [cm^{-1}]:
3060.83 (aryl-H), 3015.09 (CH_3), 2834.83 (OCH_3), 1585.10, 1495.12, 1479.48 (aryl-H), 1244.76 (C-O-C), 811.75 (1,4-disubstituation), 517.52 (Sn-C)

Elemental analysis: calculated (%) for $C_{25}H_{22}OSn$: C, 65.68; H, 4.85; found: C, 65.35; H, 4.80

VI References

[1] R. A. Alderden, M. D. Hall, T. W. Hambley; The Discovery and Development of Cisplatin; Journal of Chemical Education; vol. 83; 2006; p 728

[2] H. K. P. Koepf-Maier; Non-platinum group metal antitumor agents. History, current status, and perspectives; Chemical Reviews; vol. 87; 1987; p. 1137

[3] S. Dilruba, G. V. Kalayda; Platinum-based drugs: past, present and future; Cancer Chemotherapy and Pharmacology; vol. 77; 2016; p. 1103

[4] D. Wang, S. J. Lippard; Cellular Processing of Platinum Anticancer Drugs; Nature Reviews Drug Discovery; vol. 4; 2005; p. 307

[5] S. Tabassum, C. Pettinari; Chemical and biotechnological developments in organotin cancer chemotherapy; Journal of Organometallic Chemistry; vol. 691; 2006; p. 1761

[6] S. Hadjikakou, N. Hadjiliadis; Antiproliferative and anti-tumor activity of organotin compounds; Coordination Chemistry Reviews; vol. 253; 2009; p. 235

[7] H. Hug; Apoptose: die Selbstvernichtung der Zelle als Überlebensschutz; Biologie in unserer Zeit; 2000; p. 128

[8] M. Z. Bulatović et al.; Organotin(IV)-loaded mesoporous silica as a biocompatible strategy in cancer treatment; Angewandte Chemie International Edition Engl.; vol. 53; 2014; p. 5982

[9] G. N. Kaluđerović, R. Paschke, S. Prashar, S. Gómez-Ruiz; Synthesis, characterization and biological studies of 1-D polymeric triphenyltin(IV) carboxylates; Journal of Organometallic Chemistry; vol. 695; 2010; p. 1883

[10] D. Ghazi, Z. Rasheed, E. Yousif; A Review of Organotin Compounds: Chemistry and Applications; Archives of Organic and Inorganic Chemical Sciences (AOICS); vol. 3; 2018; p. 344

[11] Y. Ellahioui, S. Prashar, S. Gómez-Ruiz; Anticancer Applications and Recent Investigations of Metallodrugs Based on Gallium, Tin and Titanium; Inorganics; vol. 5; 2017; p. 1

[12] S. Gómez-Ruiz et al.; On the discovery, biological effects, and use of Cisplatin and metallocenes in anticancer chemotherapy; Bioinorganic Chemistry and Applications; 2012; p. 1

[13] G. N. Kaluđerović, R. Paschke; Anticancer Metallotherapeutics in Preclinical Development; Current Medicinal Chemistry; vol. 18; 2011; p. 4738

[14] G. N. Kaluđerović et al.; Synthesis and biological applications of ionic triphenyltin(IV) chloride carboxylate complexes with exceptionally high cytotoxicity; Metallomics; vol. 2; 2010; p. 419

[15] I. Predarska et al.; Triphenyltin(IV) Carboxylates with Exceptionally High Cytotoxicity against Different Breast Cancer Cell Lines; Biomolecules; vol. 13; 2023; p. 1

[16] E. Dubler, R. Buschmann, H. W. Schmalle; Isomer abundance of bis-β-diketonato complexes of titanium(IV). Crystal structures of the antitumor compound budotitane [$Ti^{IV}(bzac)_2(OEt)_2$] and of its dichloro-derivative [$Ti^{IV}(bzac)_2Cl_2$] (bzac=1-phenylbutane-1,3-dionate); Journal of Inorganic Biochemistry; vol. 95; 2003; p. 97

[17] A. Alama, B. Tasso, F. Novelli, F. Sparatore; Organometallic compounds in oncology: implications of novel organotins as antitumor agents; Drug Discovery Today; vol. 14; 2009; p. 500

[18] D. Hübner et al.; Anionic chlorido(triphenyl)tin(IV) bearing N-phthaloylglycinato or 1,2,4-benzenetricarboxylato 1,2-anhydride ligands: potential cytotoxic and apoptosis-inducing agents against several types of cancer; Chemical Biology & Drug Design; vol. 89; 2017; p. 628

[19] S. Gómez-Ruiz, T. P. Stanojković, G. N. Kaluđerović; Synthesis, characterization, biological studies and in vitro cytotoxicity on human cancer cell lines of titanium(IV) and tin(IV) derivatives with the a,a´-dimercapto-o-xylene ligand; Applied Organometallic Chemistry; vol. 26; 2012; p. 383

[20] C. C. Yammal, J. C. Podesta, R. A. Rossi; Reactions of triorganostannyl ions with haloarenes in liquid ammonia; Journal of Organometallic Chemistry; vol. 57; 1992; p. 5720

[21] H. Gilman, S. D. Rosenberg; Reaction of Triphenyltin-Lithium with organic halides; Contribution from the Chemical Laboratories of Iowa State College; 1952; p. 680

[22] S. C. Schneeweiß; Synthesis of tetrakis(4-methoxybenzene/4-methylbenzene)tin(IV) complexes; Hochschule Merseburg; 2025

[23] S. Bienz, L. Bigler, T. Fox, H. Meier; Spektroskopische Methoden in der organischen Chemie, 9 Aufl.; Thieme Verlag; Stuttgart; 2016; p. 52-59, 122-128, 168, 190, 196-199

[24] SDBS-Database; 1H-NMR Triphenyltin chloride; https://sdbs.db.aist.go.jp/HNmrSpectralView.aspx?imgdir=hsp&fname=HSP49601&sdbsno=5815; last time used 06.08.2025

[25] Sigma Aldrich; Tabelle der chemischen Verschiebungen von Verunreinigungen in der ^{1}H-NMR; https://www.sigmaaldrich.com/DE/de/technical-documents/technical-article/analytical-chemistry/nuclear-magnetic-resonance/1h-nmr-and-13c-nmr-chemical-shifts-of-impurities-chart; last time used 06.08.2025

[26] A. G. Davies; Organotin Chemistry; 2 Aufl.; Wiley-VCH; 2004; p. 21-24, 102

[27] SDBS-Database; 13C-NMR Triphenyltin chloride; https://sdbs.db.aist.go.jp/CNmrSpectralView.aspx?imgdir=cds&fname=CDS09019&sdbsno=5815; last time used 06.08.2025

[28] X. Liu; Organic Chemistry I; Kwantlen Polytechnic University Pressbooks; Surrey BC; 2021; p. 197-203

[29] F. N. Haezam, N. Awang, N. F. Kamaludin, R. Mohamad; Synthesis and cytotoxic activity of organotin(IV) diallyldithiocarbamate compounds as anticancer agent towards colon adenocarcinoma cells (HT-29); Saudi Journal of Biological Sciences; vol. 28; 2021; 3160

VII Appendix

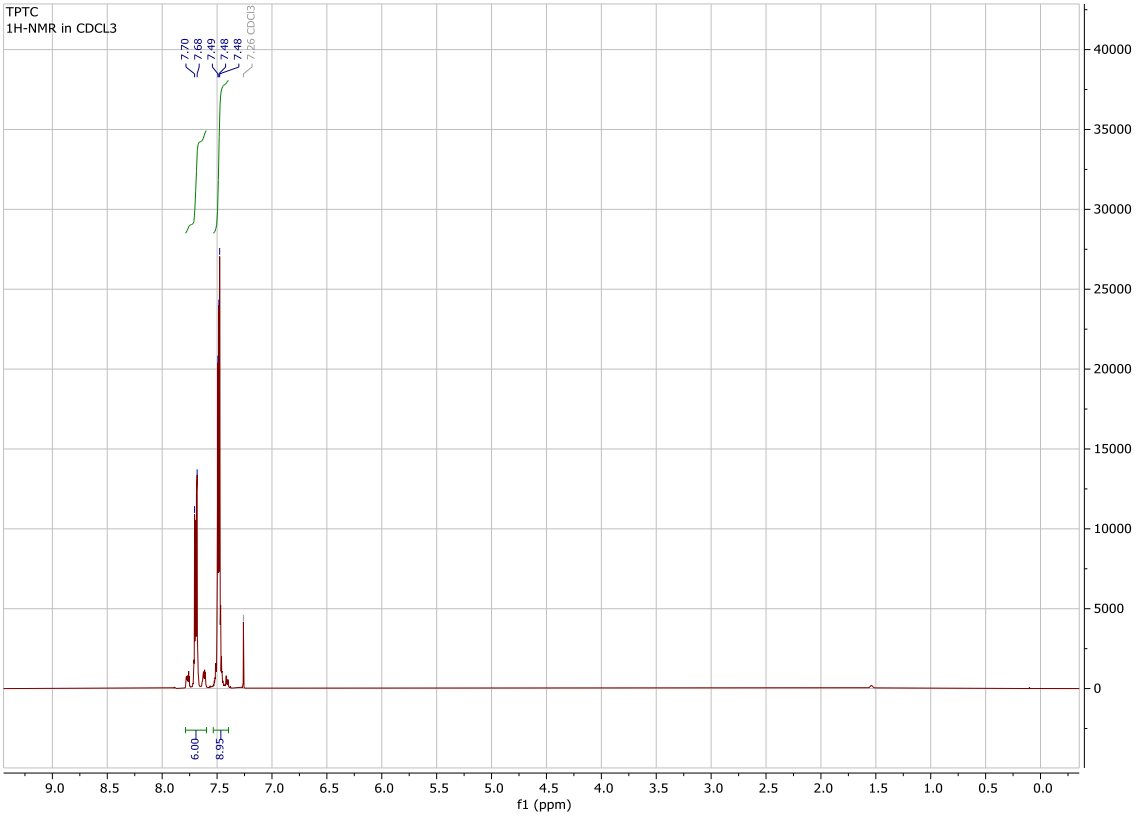

Figure A1: ^{1}H NMR spectrum of the TPTC

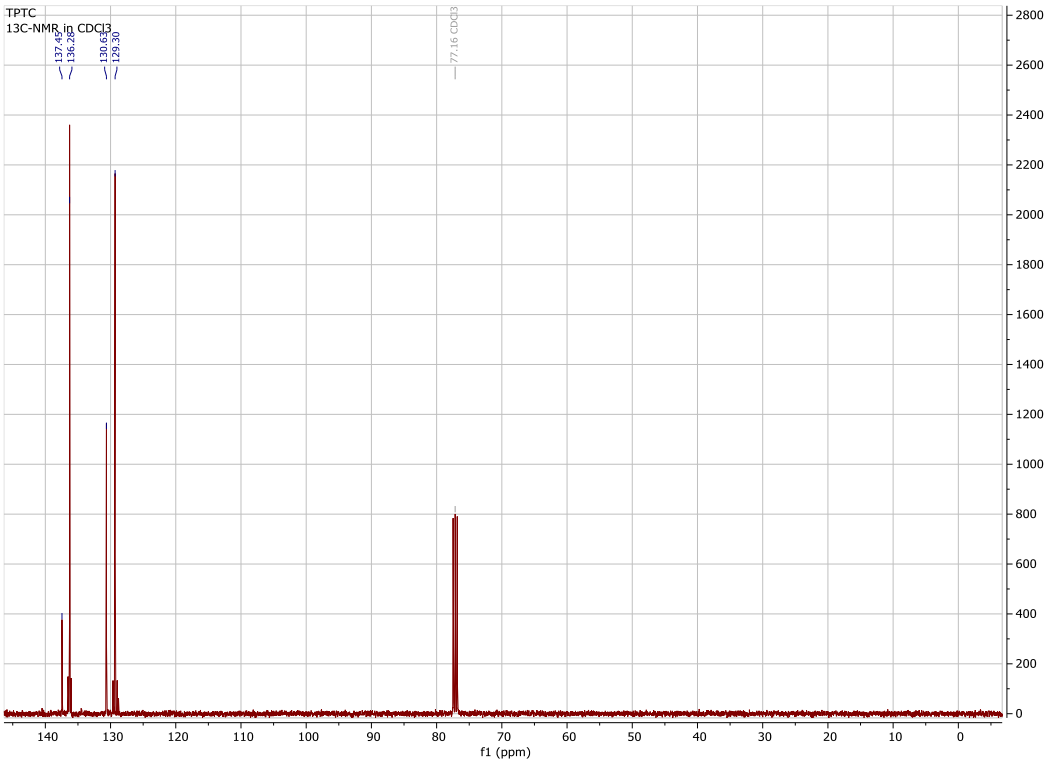

Figure A2: ^{13}C NMR spectrum of the TPTC

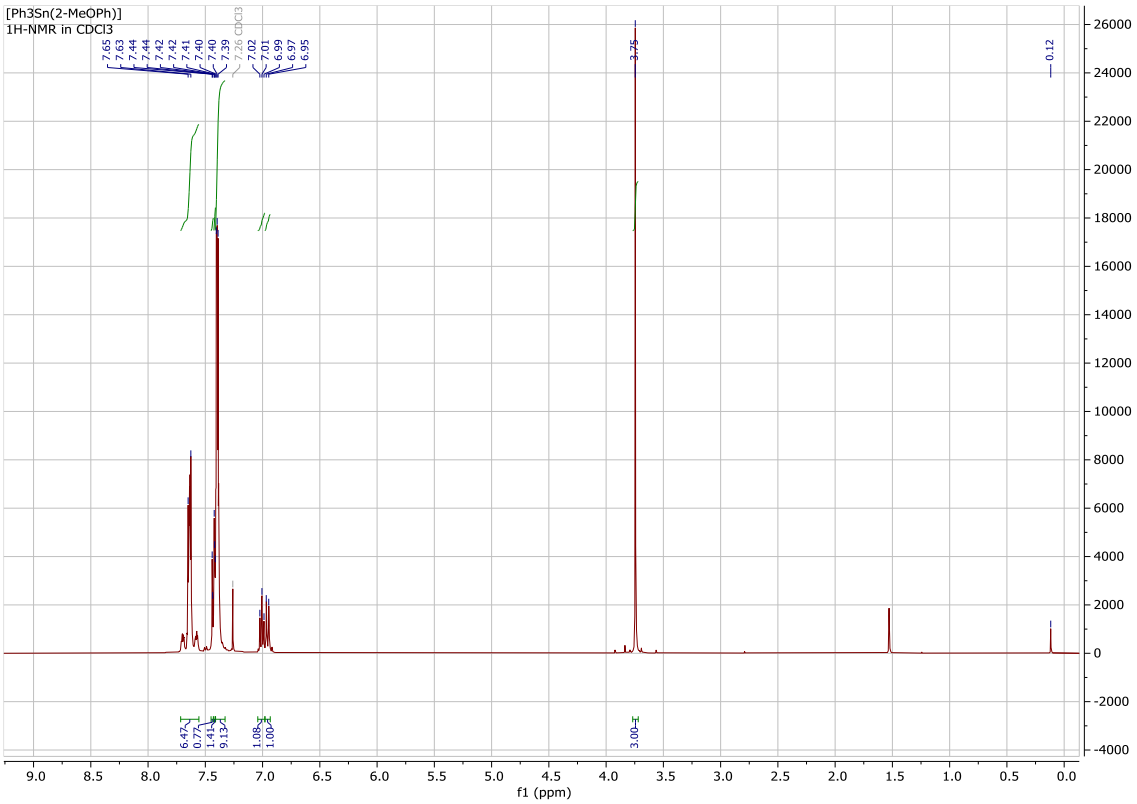

Figure A3: ^{1}H-NMR spectrum of [Ph_3Sn(2-MeOPh)]

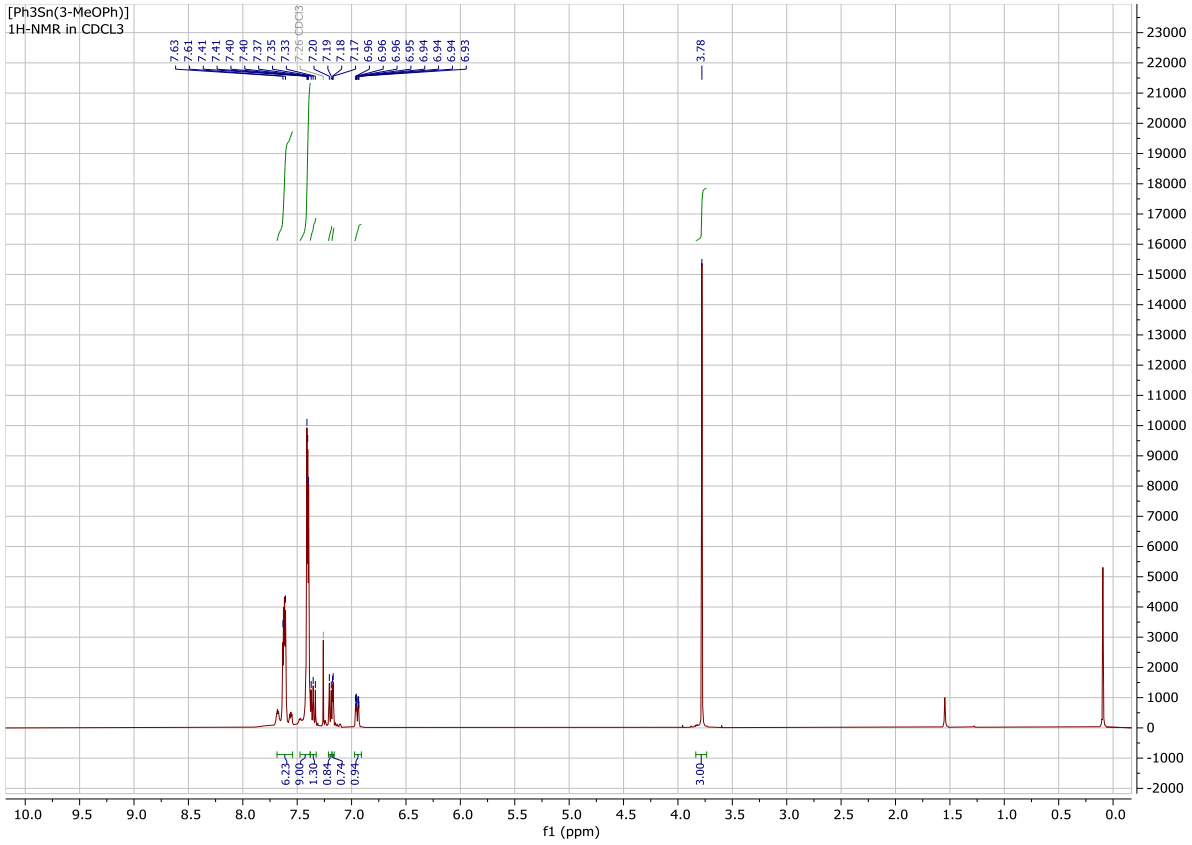

Figure A4: ^{1}H NMR spectrum of [Ph_3Sn(3-MeOPh)]

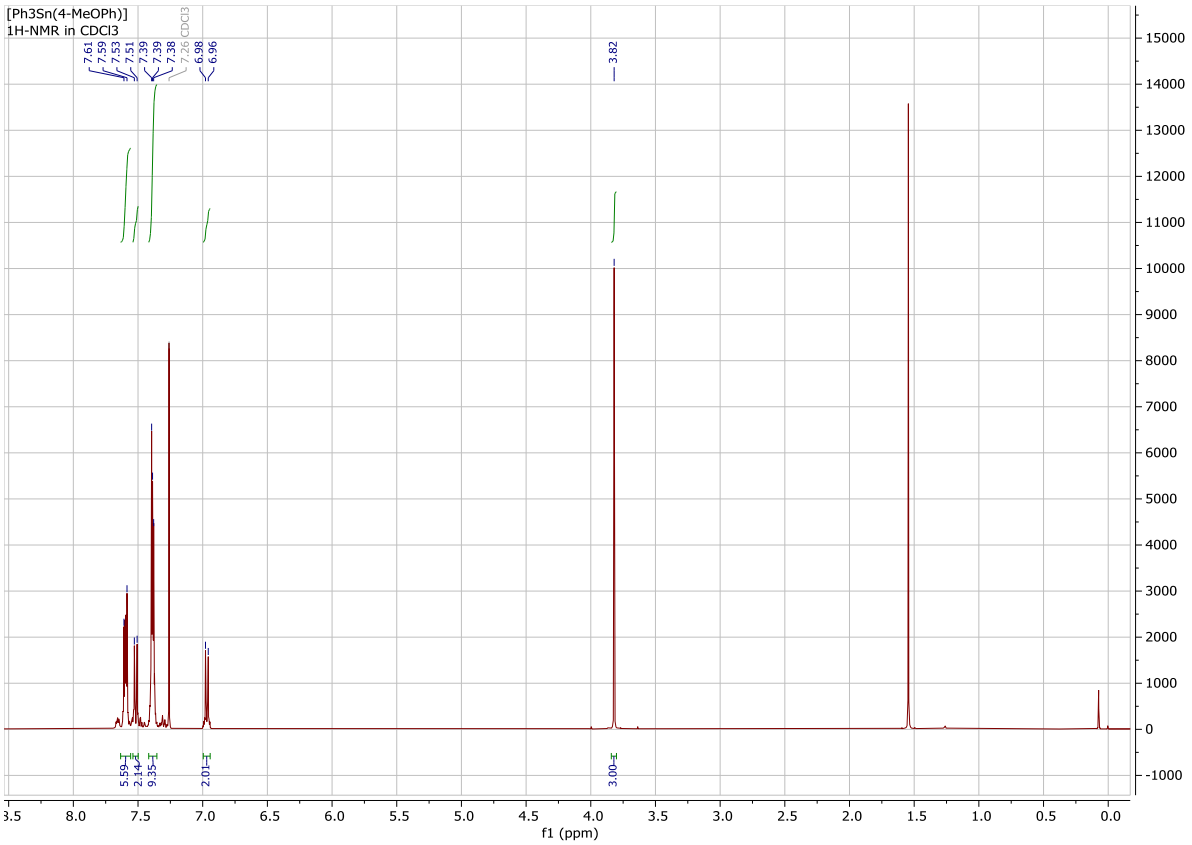

Figure A5: ^{1}H NMR spectrum of [Ph_3Sn(4-MeOPh)]

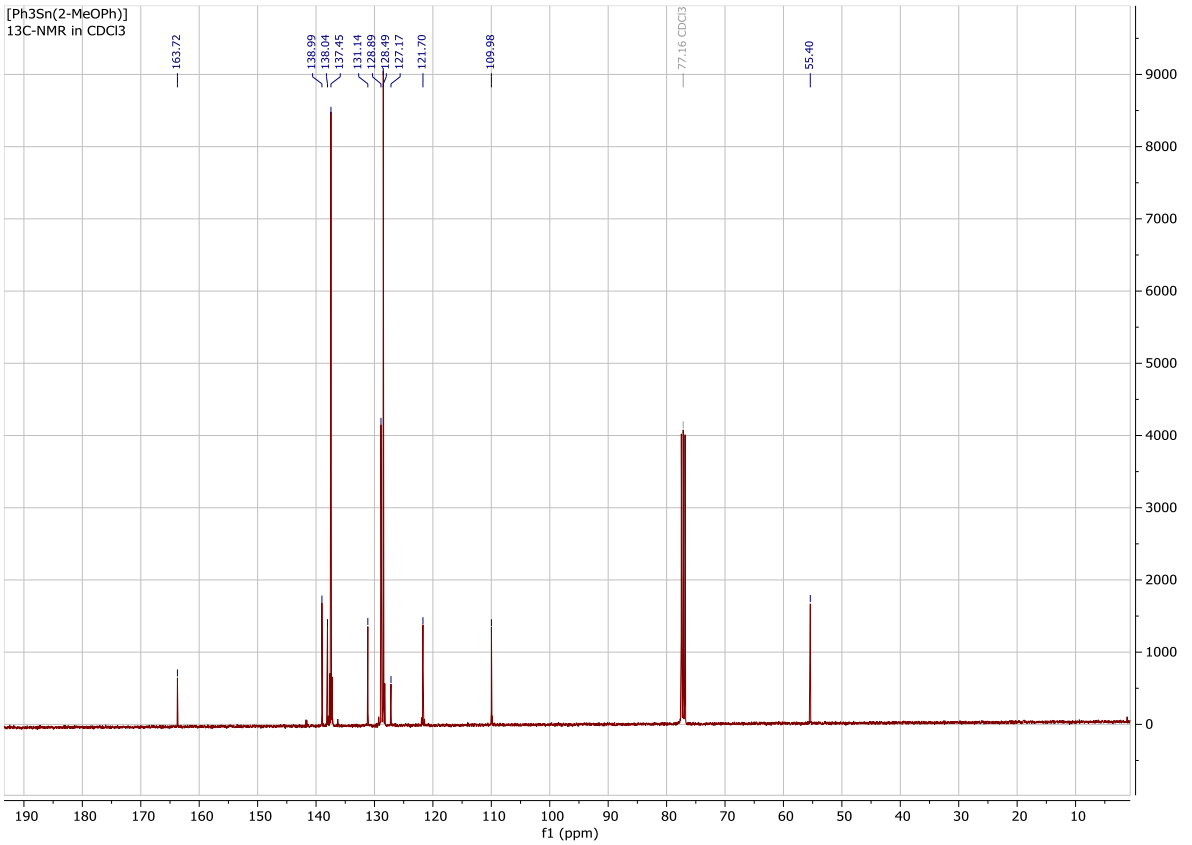

Figure A6: ^{13}C NMR spectrum of [Ph_3Sn(2-MeOPh)]

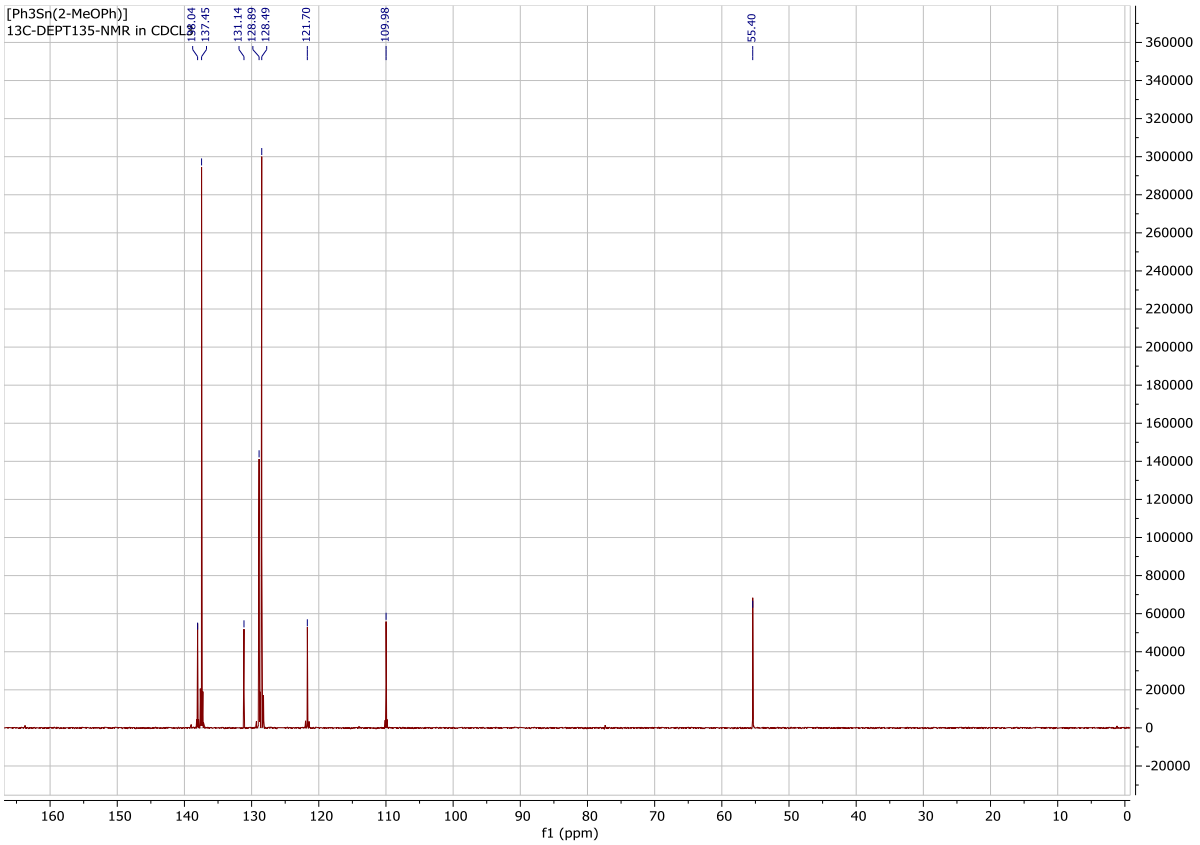

Figure A7: ^{13}C-DEPT-135-NMR spectrum of [Ph_3Sn(2-MeOPh)]

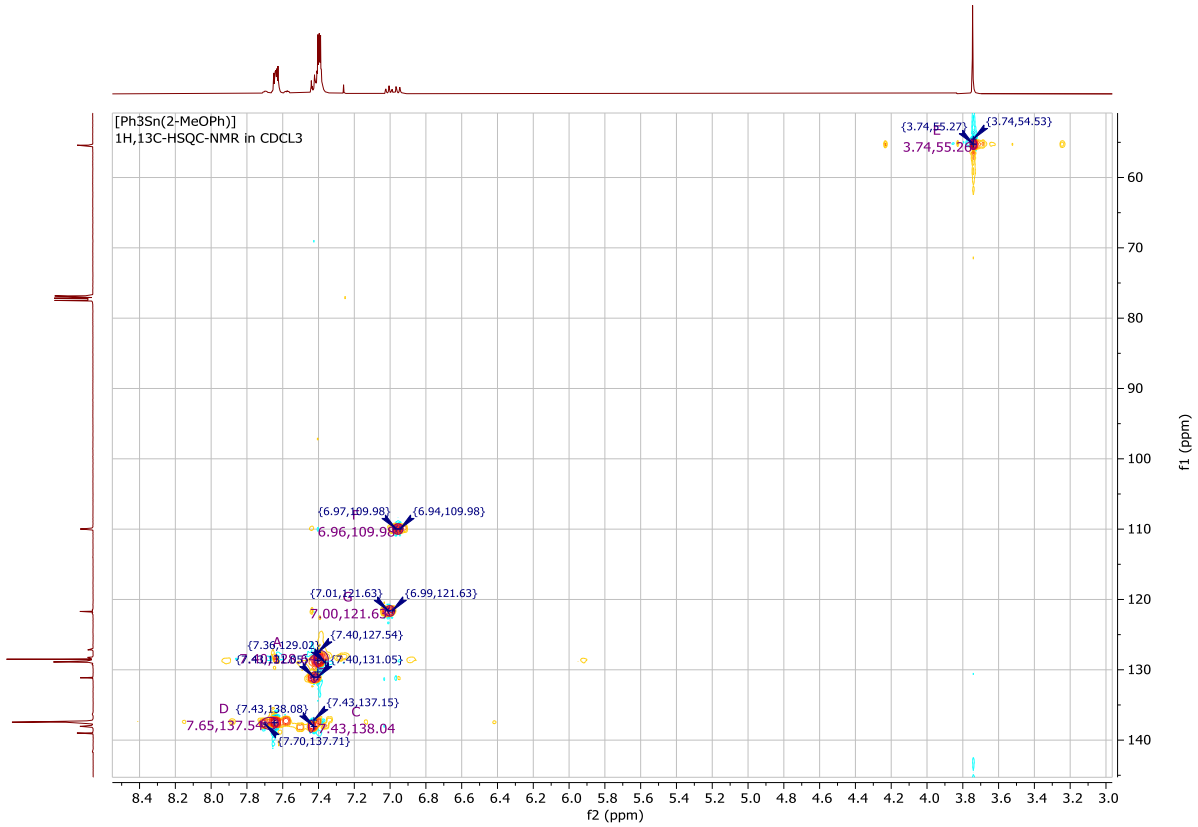

Figure A8: H,C-COSY NMR spectrum of [Ph_3Sn(2-MeOPh)]

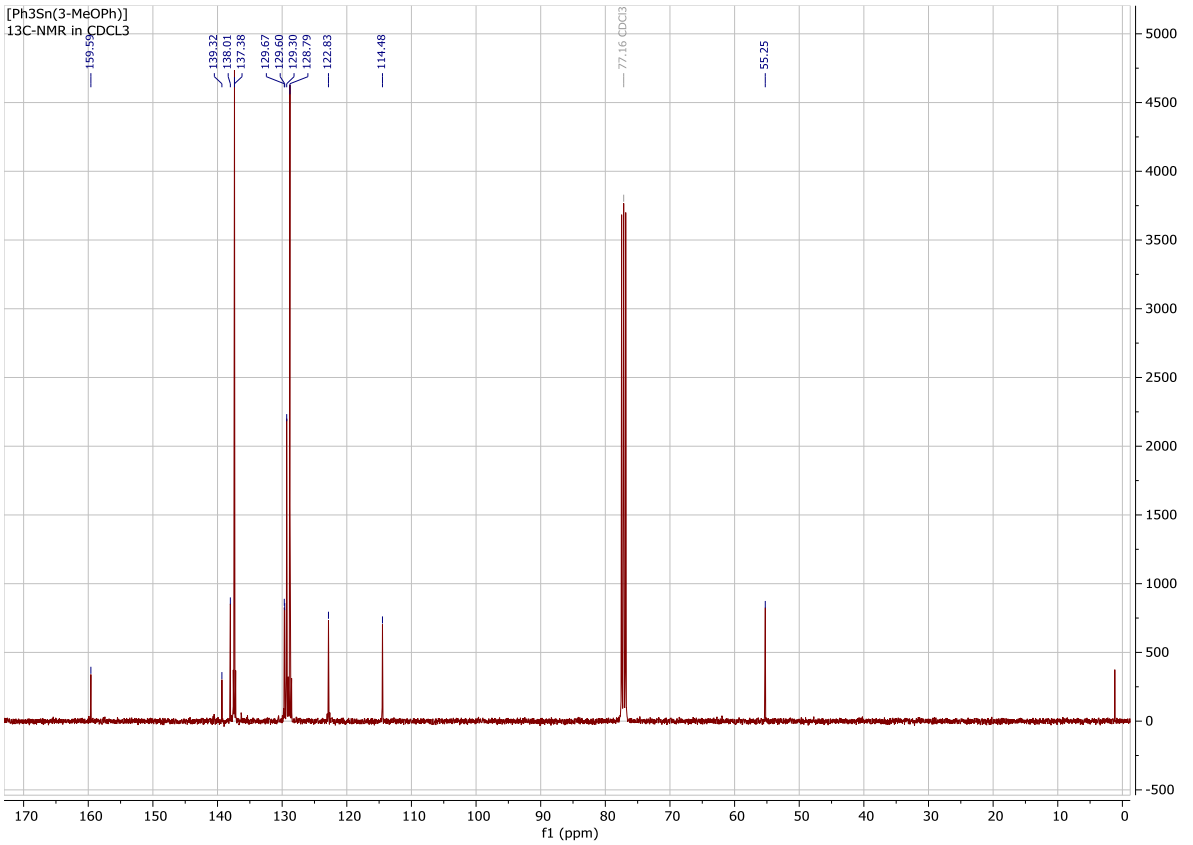

Figure A9: ^{13}C NMR spectrum of [Ph_3Sn(3-MeOPh)]

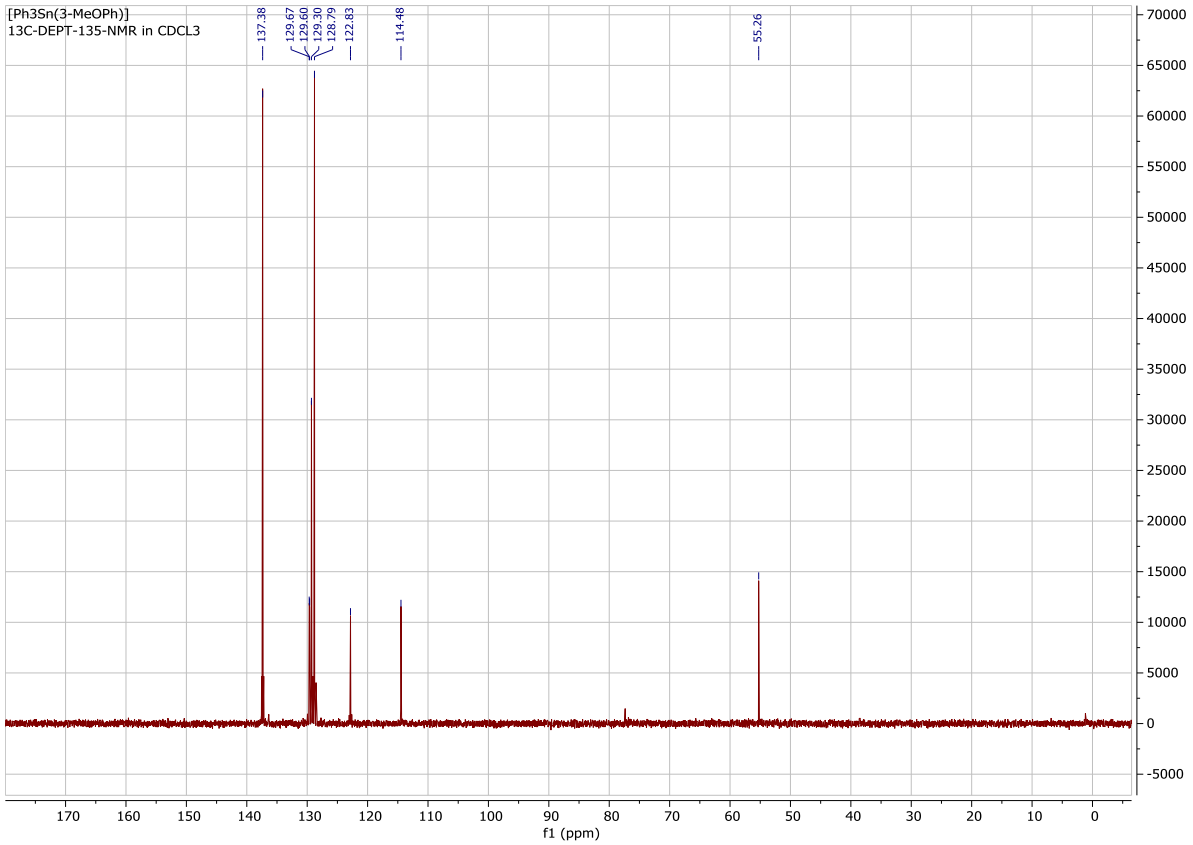

Figure A10: ^{13}C-DEPT-135-NMR spectrum of [Ph_3Sn(3-MeOPh)]

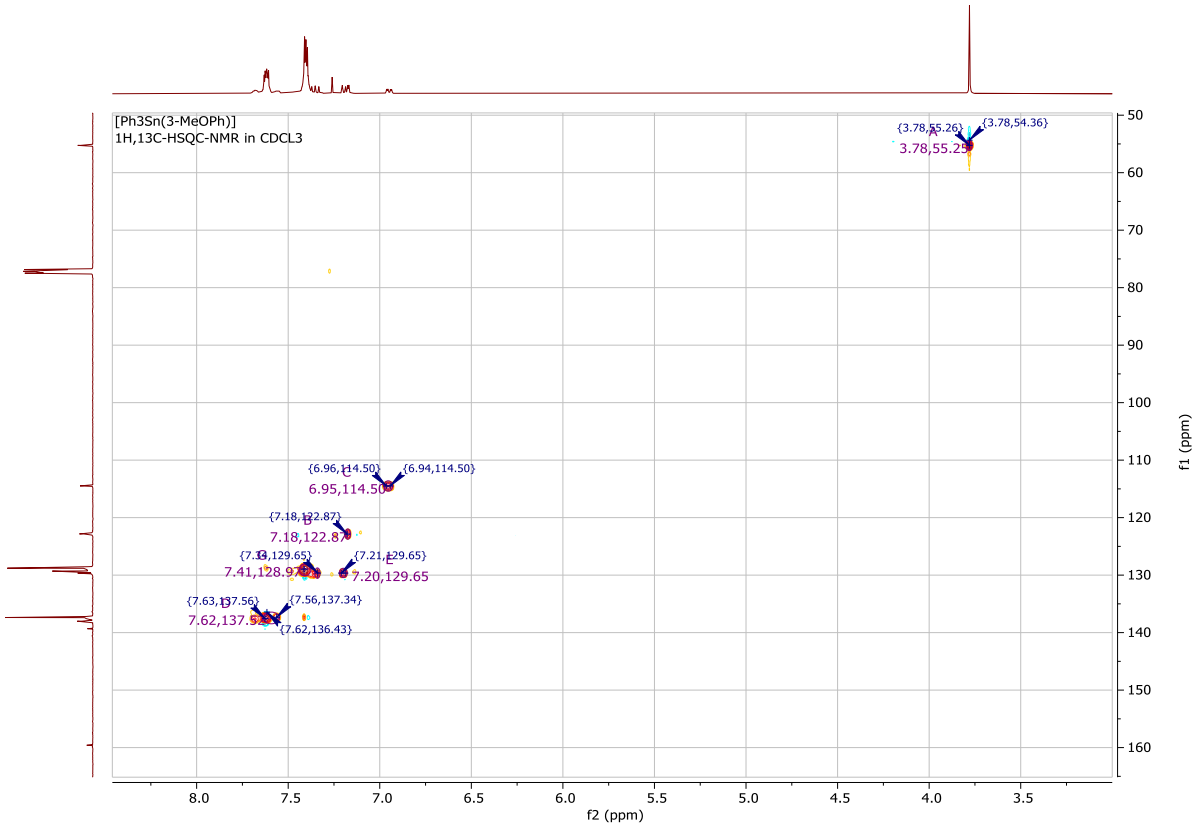

Figure A11: Complete H,C-COSY NMR spectrum of [Ph_3Sn(3-MeOPh)]

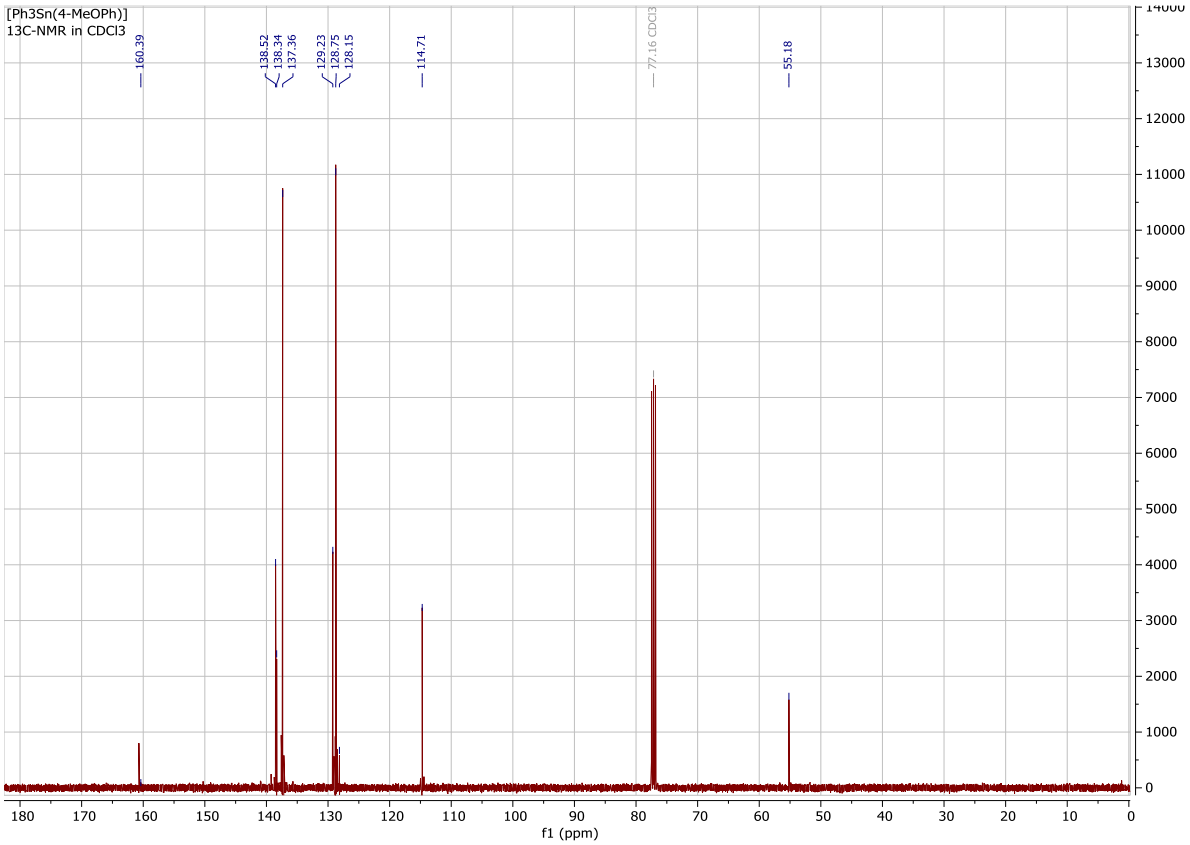

Figure A12: ^{13}C NMR spectrum of [Ph_3Sn(4-MeOPh)]

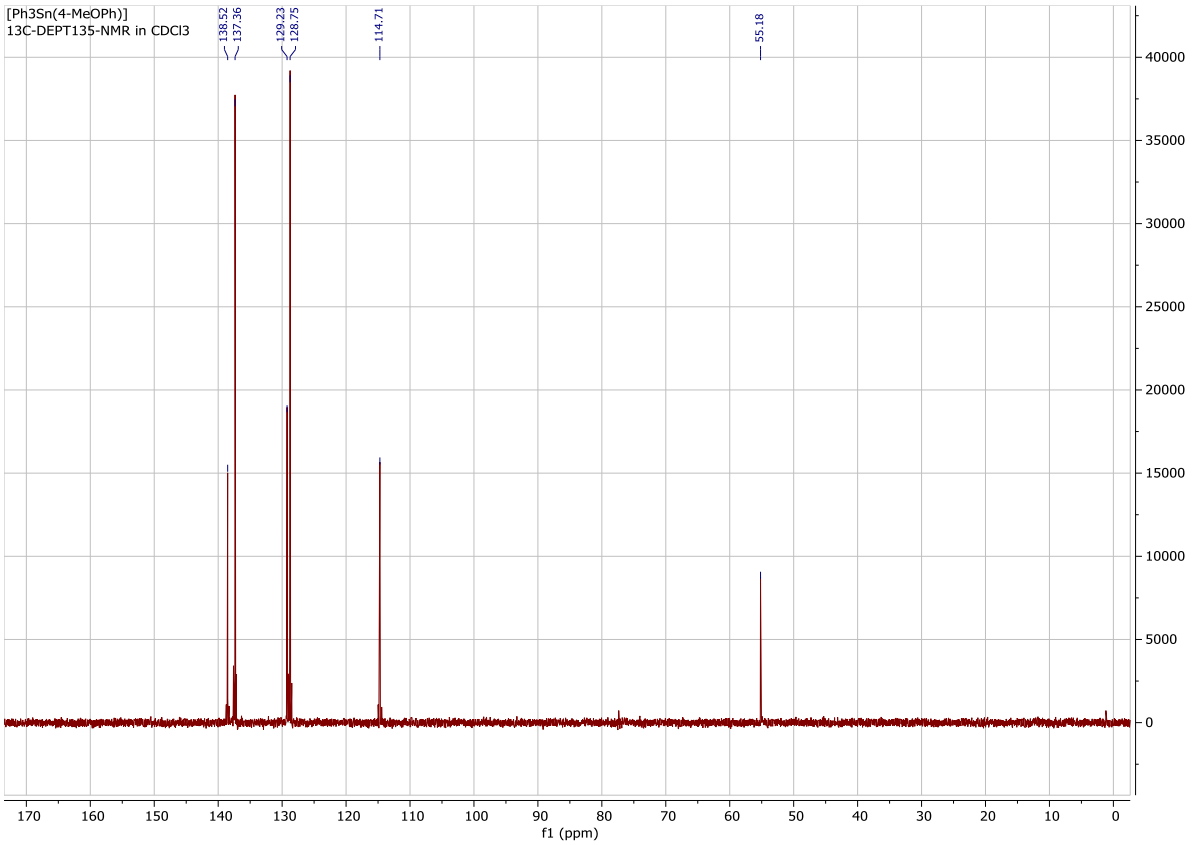

Figure A13: ^{13}C-DEPT-135-NMR spectrum of [Ph_3Sn(4-MeOPh)]

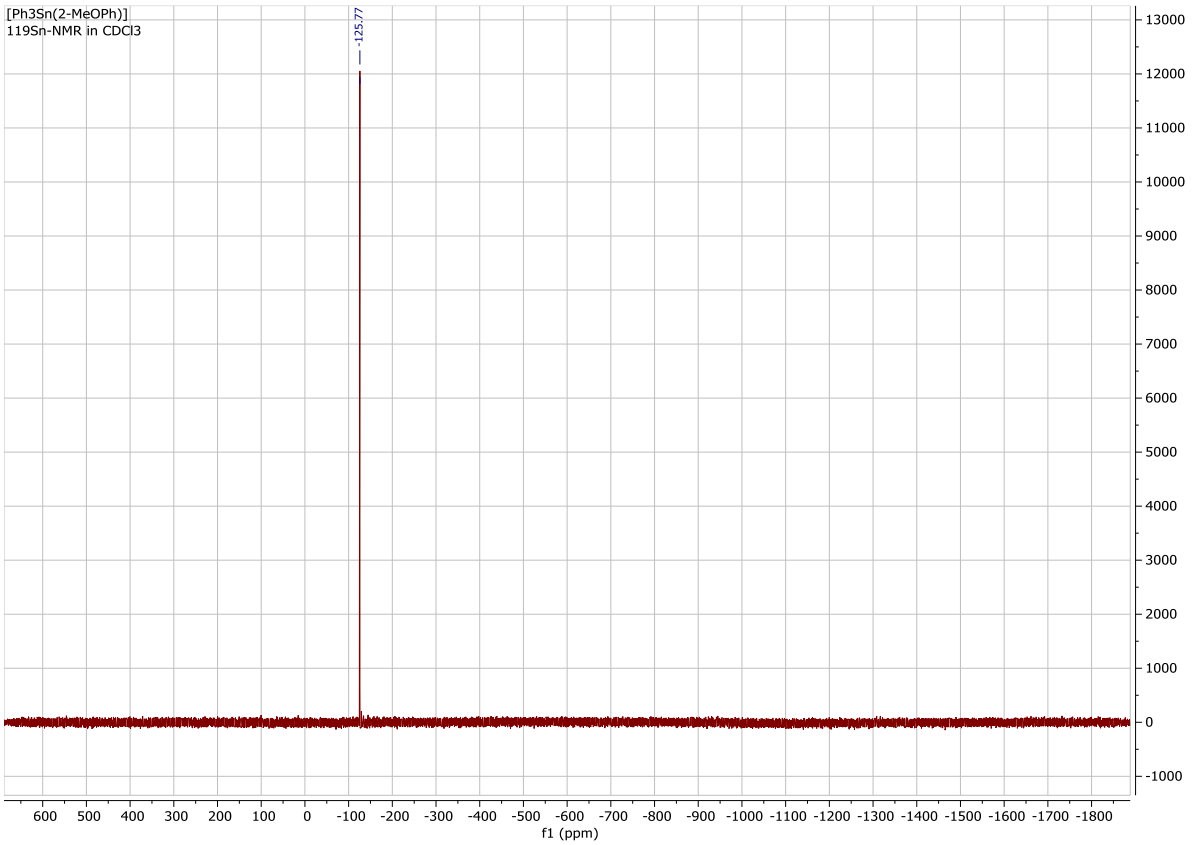

Figure A14: ^{119}Sn NMR spectrum of [Ph_3Sn(2-MeOPh)]

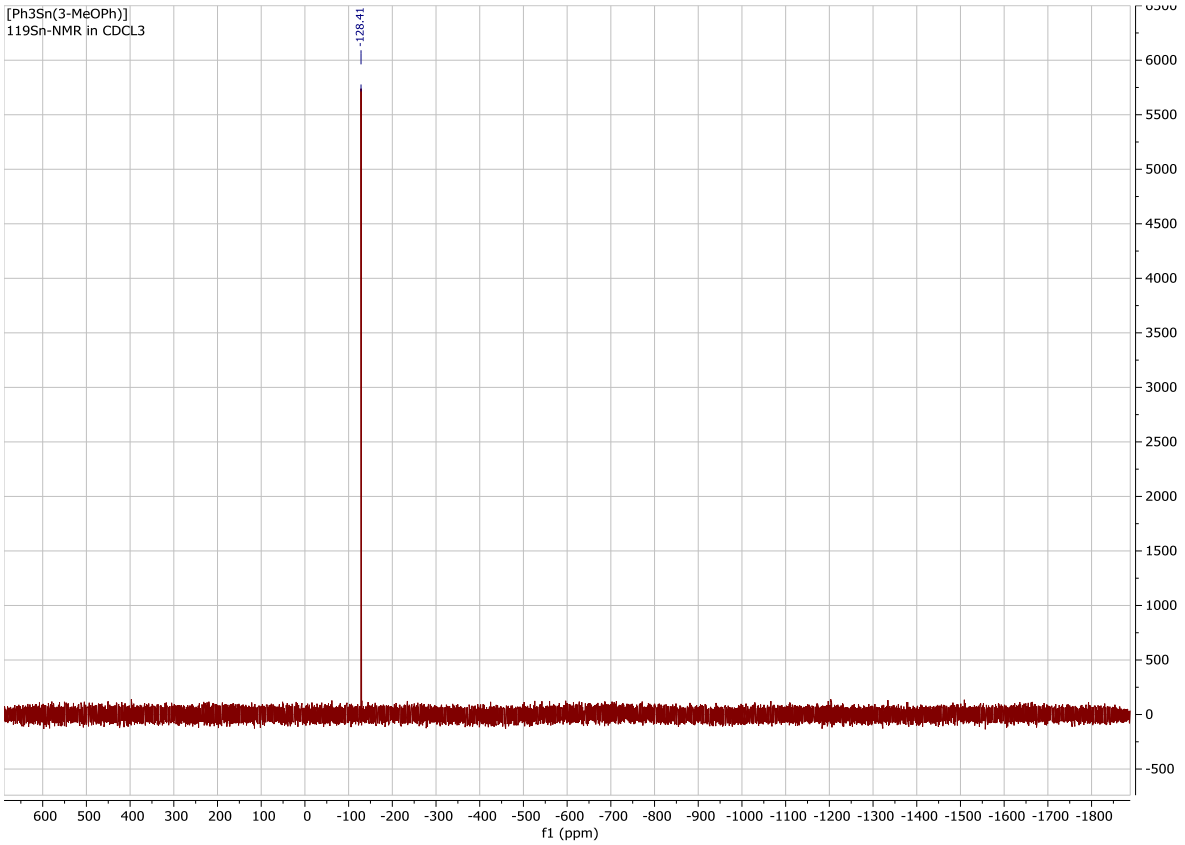

Figure A15: ^{119}Sn NMR spectrum of [Ph_3Sn(3-MeOPh)]

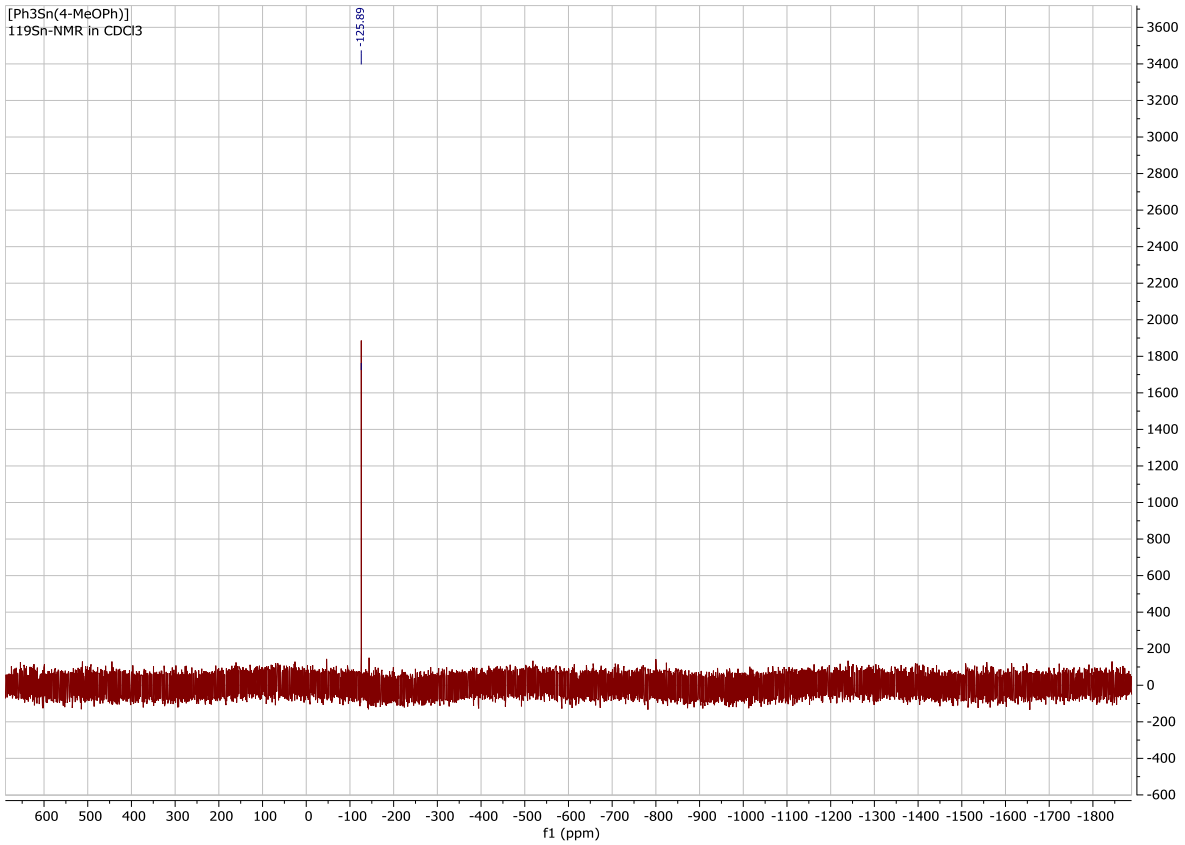

Figure A16: ^{119}Sn NMR spectrum of [Ph3Sn(4-MeOPh)]

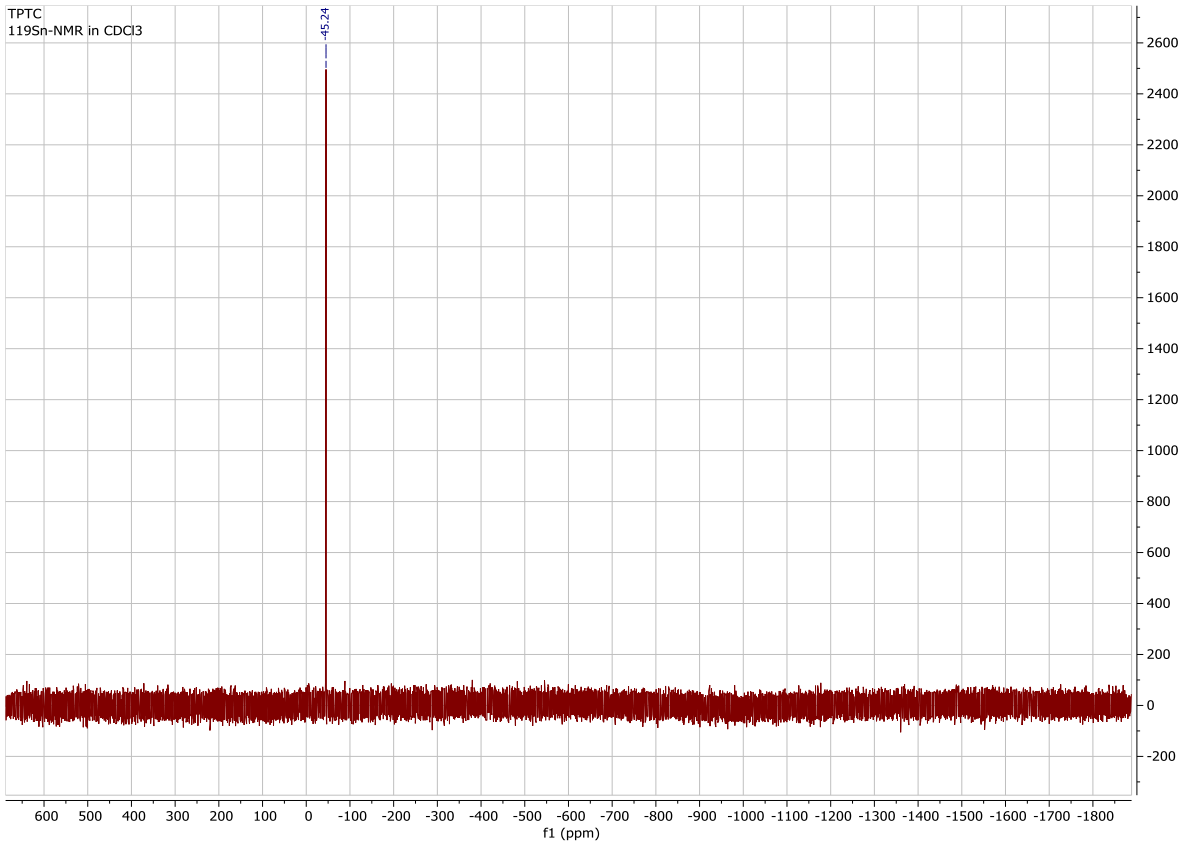

Figure A17: ^{119}Sn NMR spectrum of the TPTC

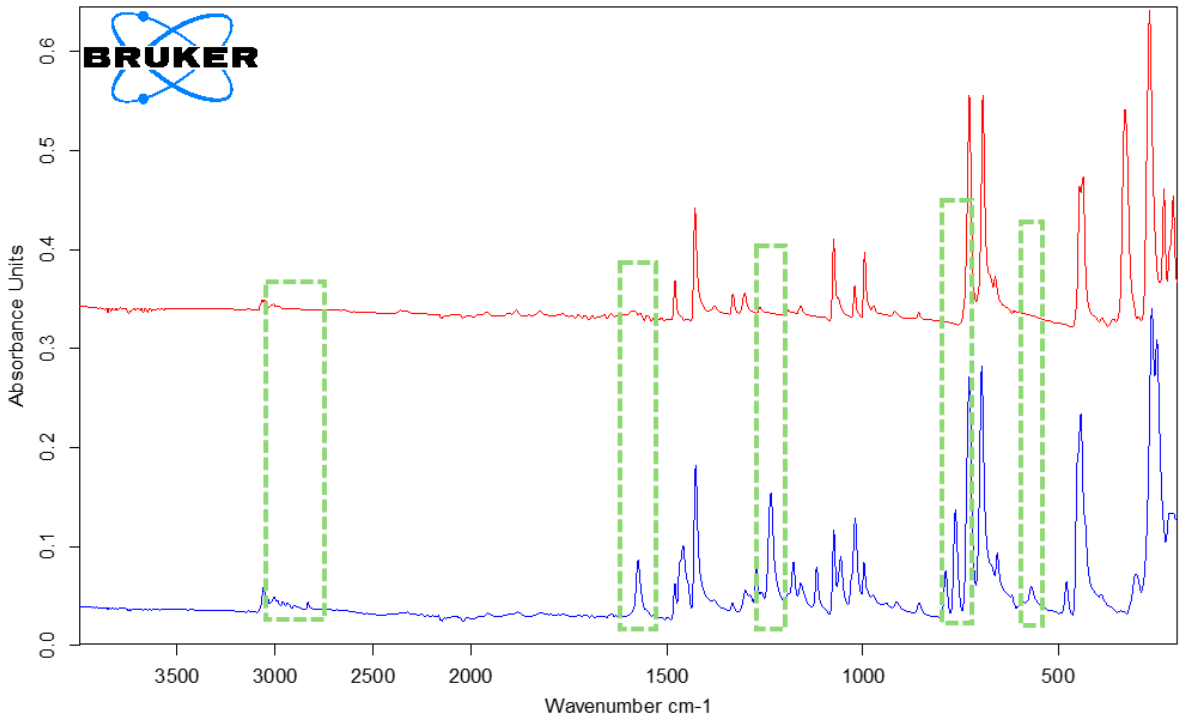

Figure A18: Comparison of the IR spectra of [Ph_3Sn(2-MeOPh)] (blue) and TPTC (red)

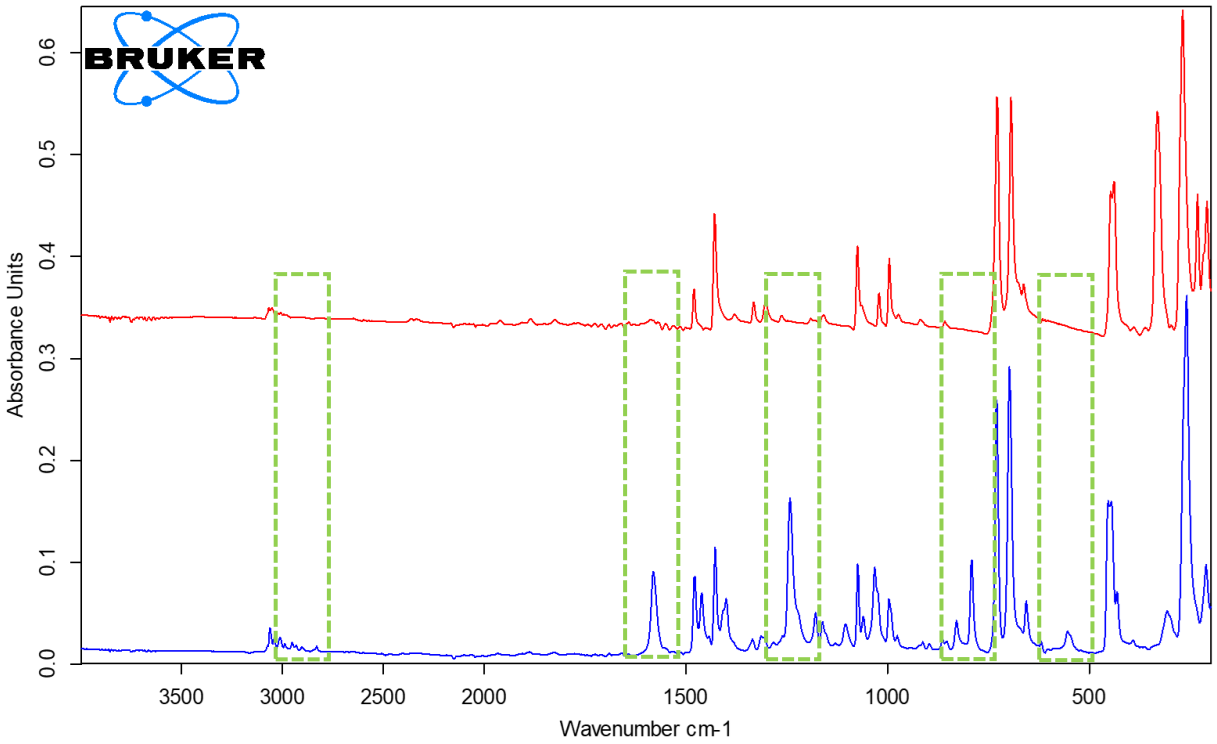

Figure A19: Comparison of the IR spectra of [Ph_3Sn(3-MeOPh)] (blue) and TPTC (red)

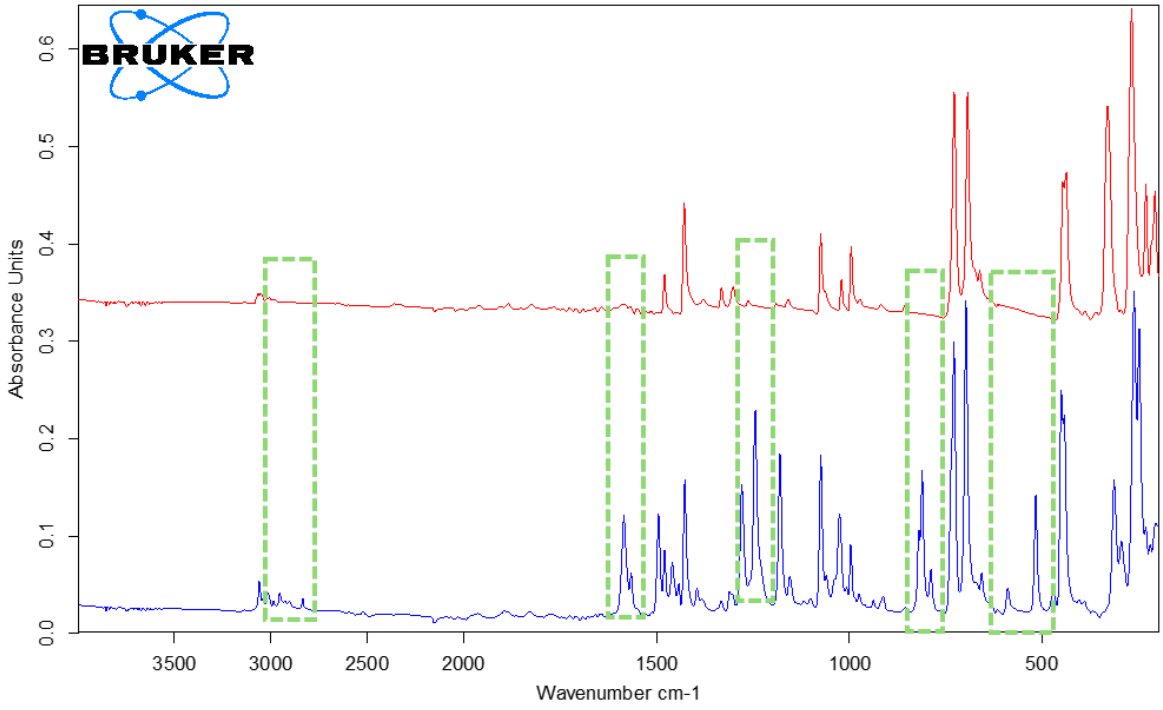

Figure A20: Comparison of the IR spectra of TPTC (red) and [Ph_3Sn(4-MeOPh)] (blue)